

---

# Learning Dynamic Belief Graphs to Generalize on Text-Based Games

---

Ashutosh Adhikari<sup>†\*</sup> Xingdi Yuan<sup>♡\*</sup> Marc-Alexandre Côté<sup>♡\*</sup>  
Mikuláš Zelinka<sup>‡</sup> Marc-Antoine Rondeau<sup>♡</sup>  
Romain Laroche<sup>♡</sup> Pascal Poupart<sup>†¶</sup> Jian Tang<sup>♦♦</sup>  
Adam Trischler<sup>♡</sup> William L. Hamilton<sup>◇♦</sup>

<sup>†</sup>University of Waterloo    <sup>♡</sup>Microsoft Research, Montréal    <sup>‡</sup>Charles University  
<sup>♦</sup>Mila    <sup>◇</sup>McGill University    <sup>♦</sup>HEC Montréal    <sup>¶</sup>Vector Institute  
eric.yuan@microsoft.com

## Abstract

Playing text-based games requires skills in processing natural language and sequential decision making. Achieving human-level performance on text-based games remains an open challenge, and prior research has largely relied on hand-crafted structured representations and heuristics. In this work, we investigate how an agent can plan and generalize in text-based games using graph-structured representations learned end-to-end from raw text. We propose a novel graph-aided transformer agent (GATA) that infers and updates latent *belief graphs* during planning to enable effective action selection by capturing the underlying game dynamics. GATA is trained using a combination of reinforcement and self-supervised learning. Our work demonstrates that the learned graph-based representations help agents converge to better policies than their text-only counterparts and facilitate effective generalization across game configurations. Experiments on 500+ unique games from the TextWorld suite show that our best agent outperforms text-based baselines by an average of 24.2%.

## 1 Introduction

Text-based games are complex, interactive simulations in which the game state is described with text and players act using simple text commands (e.g., `light torch with match`). They serve as a proxy for studying how agents can exploit language to comprehend and interact with the environment. Text-based games are a useful challenge in the pursuit of intelligent agents that communicate with humans (e.g., in customer service systems).

Solving text-based games requires a combination of reinforcement learning (RL) and natural language processing (NLP) techniques. However, inherent challenges like partial observability, long-term dependencies, sparse rewards, and combinatorial action spaces make these games very difficult.<sup>2</sup> For instance, Hausknecht et al. [16] show that a state-of-the-art model achieves a mere 2.56% of the total possible score on a curated set of text-based games for human players [5]. On the other hand, while text-based games exhibit many of the same difficulties as linguistic tasks like open-ended dialogue, they are more structured and constrained.

To design successful agents for text-based games, previous works have relied largely on heuristics that exploit games' inherent structure. For example, several works have proposed rule-based components

---

\* Equal contribution.

<sup>2</sup>We challenge readers to solve this representative game: <https://aka.ms/textworld-tryit>.

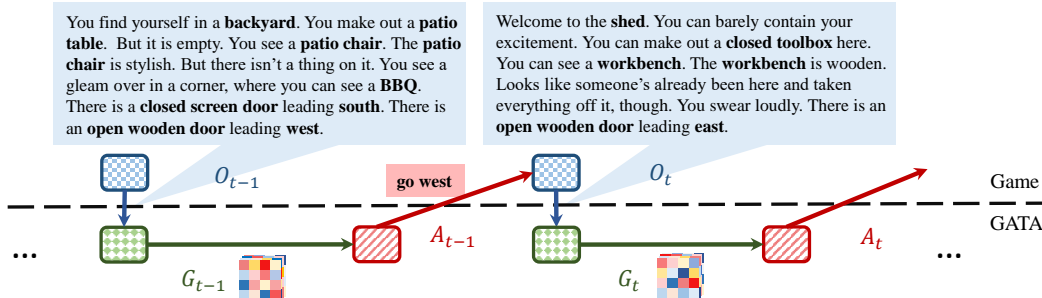


Figure 1: GATA playing a text-based game by updating its belief graph. In response to action  $A_{t-1}$ , the environment returns text observation  $O_t$ . Based on  $O_t$  and  $G_{t-1}$ , the agent updates  $G_t$  and selects a new action  $A_t$ . In the figure, blue box with squares is the game engine, green box with diamonds is the graph updater, red box with slashes is the action selector.

that prune the action space or shape the rewards according to *a priori* knowledge of the game dynamics [50, 24, 1, 48]. More recent approaches take advantage of the graph-like structure of text-based games by building knowledge graph (KG) representations of the game state: Ammanabrolu and Riedl [4], Ammanabrolu and Hausknecht [3], for example, use hand-crafted heuristics to populate a KG that feeds into a deep neural agent to inform its policy. Despite progress along this line, we expect more general, effective representations for text-based games to arise in agents that learn and scale more automatically, which replace heuristics with learning [37].

This work investigates how we can learn graph-structured state representations for text-based games in an entirely data-driven manner. We propose the graph aided transformer agent (GATA)<sup>3</sup> that, in lieu of heuristics, *learns* to construct and update graph-structured beliefs<sup>4</sup> and use them to further optimize rewards. We introduce two self-supervised learning strategies—based on text reconstruction and mutual information maximization—which enable our agent to learn latent graph representations without direct supervision or hand-crafted heuristics.

We benchmark GATA on 500+ unique games generated by TextWorld [9], evaluating performance in a setting that requires generalization across different game configurations. We show that GATA outperforms strong baselines, including text-based models with recurrent policies. In addition, we compare GATA to agents with access to ground-truth graph representations of the game state. We show that GATA achieves competitive performance against these baselines even though it receives only partial text observations of the state. Our findings suggest, promisingly, that graph-structured representations provide a useful inductive bias for learning and generalizing in text-based games, and act as a memory enabling agents to optimize rewards in a partially observed setting.

## 2 Background

**Text-based Games:** Text-based games can be formally described as partially observable Markov decision processes (POMDPs) [9]. They are environments in which the player receives text-only observations  $O_t$  (these describe the observable state, typically only partially) and interacts by issuing short text phrases as actions  $A_t$  (e.g., in Figure 1, *go west* moves the player to a new location). Often, the end goal is not clear from the start; the agent must infer the objective by earning sparse rewards for completing subgoals. Text-based games have a variety of difficulty levels determined mainly by the environment’s complexity (i.e., how many locations in the game, and how many objects are interactive), the game length (i.e., optimally, how many actions are required to win), and the verbosity (i.e., how much text information is irrelevant to solving the game).

**Problem Setting:** We use TextWorld [9] to generate unique *choice-based* games of varying difficulty. All games share the same overarching theme: an agent must gather and process cooking ingredients, placed randomly across multiple locations, according to a recipe it discovers during the game. The agent earns a point for collecting each ingredient and for processing it correctly. The game is won

<sup>3</sup>Code and dataset used: <https://github.com/xingdi-eric-yuan/GATA-public>

<sup>4</sup>Text-based games are partially observable environments.

upon completing the recipe. Processing any ingredient incorrectly terminates the game (e.g., `slice carrot` when the recipe asked for a `diced carrot`). To process ingredients, an agent must find and use appropriate tools (e.g., a knife to `slice`, `dice`, or `chop`; a stove to `fry`, an oven to `roast`).

We divide generated games, all of which have unique recipes and map configurations, into sets for training, validation, and test. Adopting the supervised learning paradigm for evaluating generalization, we tune hyperparameters on the validation set and report performance on a test set of previously unseen games. Testing agents on unseen games (within a difficulty level) is uncommon in prior RL work, where it is standard to train and test on a single game instance. Our approach enables us to measure the robustness of learned policies as they generalize (or fail to) across a “distribution” of related but distinct games. Throughout the paper, we use the term *generalization* to imply the ability of a single policy to play a distribution of related games (within a particular difficulty level).

**Graphs and Text-based Games:** We expect graph-based representations to be effective for text-based games because the state in these games adheres to a graph-like structure. The essential content in most observations of the environment corresponds either to entity attributes (e.g., the state of the `carrot` is `sliced`) or to relational information about entities in the environment (e.g., the `kitchen` is `north_of` the `bedroom`). This information is naturally represented as a dynamic graph  $\mathcal{G}_t = (\mathcal{V}_t, \mathcal{E}_t)$ , where the vertices  $\mathcal{V}_t$  represent entities (including the player, objects, and locations) and their current conditions (e.g., closed, fried, sliced), while the edges  $\mathcal{E}_t$  represent relations between entities (e.g., `north_of`, `in`, `is`) that hold at a particular time-step  $t$ . By design, in fact, the full state of any game generated by TextWorld can be represented explicitly as a graph of this type [53]. The aim of our model, GATA, is to estimate the game state by learning to build graph-structured beliefs from raw text observations. In our experiments, we benchmark GATA against models with direct access to the ground-truth game state rather than GATA’s noisy estimate thereof inferred from text.

### 3 Graph Aided Transformer Agent (GATA)

In this section, we introduce GATA, a novel transformer-based neural agent that can infer a graph-structured belief state and use that state to guide action selection in text-based games. As shown in Figure 2, the agent consists of two main modules: a graph updater and an action selector.<sup>5</sup> At game step  $t$ , the graph updater extracts relevant information from text observation  $O_t$  and updates its belief graph  $\mathcal{G}_t$  accordingly. The action selector issues action  $A_t$  conditioned on  $O_t$  and the belief graph  $\mathcal{G}_t$ . Figure 1 illustrates the interaction between GATA and a text-based game.

#### 3.1 Belief Graph

We denote by  $\mathcal{G}$  a belief graph representing the agent’s belief about the true game state according to what it has observed so far. We instantiate  $\mathcal{G} \in [-1, 1]^{\mathcal{R} \times \mathcal{N} \times \mathcal{N}}$  as a real-valued adjacency tensor, where  $\mathcal{R}$  and  $\mathcal{N}$  indicate the number of relation types and entities. Each entry  $\{r, i, j\}$  in  $\mathcal{G}$  indicates the strength of an inferred relationship  $r$  from entity  $i$  to entity  $j$ . We select  $\mathcal{R} = 10$  and  $\mathcal{N} = 99$  to match the maximum number of relations and entities in our TextWorld-generated games. In other words, we assume that GATA has access to the *vocabularies* of possible relations and entities but it must learn the structure among these objects, and their semantics, from scratch.

#### 3.2 Graph Updater

The graph updater constructs and updates the dynamic belief graph  $\mathcal{G}$  from text observations  $O_t$ . Rather than generating the entire belief graph at each step  $t$ , we generate a graph update,  $\Delta g_t$ , that represents the change of the agent’s belief after receiving a new observation. This is motivated by the fact that observations  $O_t$  typically communicate only incremental information about the state’s change from time step  $t - 1$  to  $t$ . The relation between  $\Delta g_t$  and  $\mathcal{G}$  is given by

$$\mathcal{G}_t = \mathcal{G}_{t-1} \oplus \Delta g_t, \tag{1}$$

<sup>5</sup>The graph updater and action selector share some structures but not their parameters (unless specified).

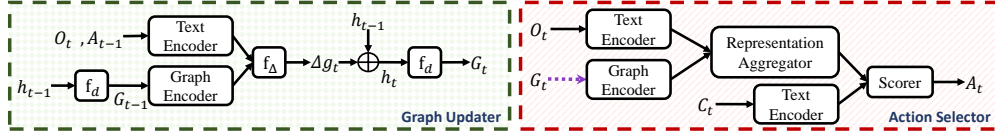


Figure 2: GATA in detail. The coloring scheme is same as in Figure 1. The **graph updater** first generates  $\Delta g_t$  using  $\mathcal{G}_{t-1}$  and  $O_t$ . Afterwards the **action selector** uses  $O_t$  and the updated graph  $\mathcal{G}_t$  to select  $A_t$  from the list of action candidates  $C_t$ . Purple dotted line indicates a detached connection (i.e., no back-propagation through such connection).

where  $\oplus$  is a graph operation function that produces the new belief graph  $\mathcal{G}_t$  given  $\mathcal{G}_{t-1}$  and  $\Delta g_t$ . We formulate the graph operation function  $\oplus$  using a recurrent neural network (e.g., a GRU [8]) as:

$$\begin{aligned}\Delta g_t &= f_\Delta(h_{\mathcal{G}_{t-1}}, h_{O_t}, h_{A_{t-1}}); \\ h_t &= \text{RNN}(\Delta g_t, h_{t-1}); \\ \mathcal{G}_t &= f_d(h_t).\end{aligned}\quad (2)$$

The function  $f_\Delta$  aggregates the information in  $\mathcal{G}_{t-1}$ ,  $A_{t-1}$ , and  $O_t$  to generate the graph update  $\Delta g_t$ .  $h_{\mathcal{G}_{t-1}}$  denotes the representation of  $\mathcal{G}_{t-1}$  from the graph encoder.  $h_{O_t}$  and  $h_{A_{t-1}}$  are outputs of the text encoder (refer to Figure 2, left part). The vector  $h_t$  is a recurrent hidden state from which we decode the adjacency tensor  $\mathcal{G}_t$ ;  $h_t$  acts as a memory that carries information across game steps—a crucial function for solving POMDPs [15]. The function  $f_d$  is a multi-layer perceptron (MLP) that decodes the recurrent state  $h_t$  into a real-valued adjacency tensor (i.e., the belief graph  $\mathcal{G}_t$ ). We elaborate on each of the sub-modules in Appendix A.

**Training the Graph Updater:** We pre-train the graph updater using two self-supervised training regimes to learn structured game dynamics. After pre-training, the graph updater is fixed during GATA’s interaction with games; at this time it provides belief graphs  $\mathcal{G}$  to the action selector. We train the action selector subsequently via RL. Both pre-training tasks share the same goal: to ensure that  $\mathcal{G}_t$  encodes sufficient information about the environment state at game step  $t$ . For training data, we gather a collection of transitions by following walkthroughs in *FTWP* games.<sup>6</sup> To ensure variety in the training data, we also randomly sample trajectories off the optimal path. Next we describe our pre-training approaches for the graph updater.

- **Observation Generation (OG):** Our first approach to pre-train the graph updater involves training a decoder model to reconstruct text observations from the belief graph. Conditioned on the belief graph,  $\mathcal{G}_t$ , and the action performed at the previous game step,  $A_{t-1}$ , the observation generation task aims to reconstruct  $O_t = \{O_t^1, \dots, O_t^{L_{O_t}}\}$  token by token, where  $L_{O_t}$  is the length of  $O_t$ . We formulate this task as a sequence-to-sequence (Seq2Seq) problem and use a transformer-based model [43] to generate the output sequence. Specifically, conditioned on  $\mathcal{G}_t$  and  $A_{t-1}$ , the transformer decoder predicts the next token  $O_t^i$  given  $\{O_t^1, \dots, O_t^{i-1}\}$ . We train the Seq2Seq model using teacher-forcing to optimize the negative log-likelihood loss:

$$\mathcal{L}_{\text{OG}} = - \sum_{i=1}^{L_{O_t}} \log p_{\text{OG}}(O_t^i | O_t^1, \dots, O_t^{i-1}, \mathcal{G}_t, A_{t-1}), \quad (3)$$

where  $p_{\text{OG}}$  is the conditional distribution parametrized by the observation generation model.

- **Contrastive Observation Classification (COC):** Inspired by the literature on contrastive representation learning [41, 19, 44, 7], we reformulate OG mentioned above as a contrastive prediction task. We use contrastive learning to maximize mutual information between the predicted  $\mathcal{G}_t$  and the text observations  $O_t$ . Specifically, we train the model to differentiate between representations corresponding to true observations  $O_t$  and “corrupted” observations  $\tilde{O}_t$ , conditioned on  $\mathcal{G}_t$  and  $A_{t-1}$ . To obtain corrupted observations, we sample randomly from the set of all collected observations across our pre-training data. We use a noise-contrastive objective and minimize the binary cross-entropy (BCE) loss given by

$$\mathcal{L}_{\text{COC}} = \frac{1}{K} \sum_{t=1}^K (\mathbb{E}_{O_t} [\log \mathcal{D}(h_{O_t}, h_{\mathcal{G}_t})] + \mathbb{E}_{\tilde{O}_t} [\log (1 - \mathcal{D}(h_{\tilde{O}_t}, h_{\mathcal{G}_t}))]). \quad (4)$$

<sup>6</sup>This is an independent and unique set of TextWorld games [39]. Details are provided in Appendix F.

Here,  $K$  is the length of a trajectory as we sample a positive and negative pair at each step and  $\mathcal{D}$  is a *discriminator* that differentiates between positive and negative samples. The motivation behind contrastive unsupervised training is that one does not require to train complex decoders. Specifically, compared to OG, the COC’s objective relaxes the need for learning syntactical or grammatical features and allows GATA to focus on learning the semantics of the  $O_t$ .

We provide further implementation level details on both these self-supervised objectives in Appendix B.

### 3.3 Action Selector

The graph updater discussed in the previous section defines a key component of GATA that enables the model to maintain a structured belief graph based on text observations. The second key component of GATA is the *action selector*, which uses the belief graph  $\mathcal{G}_t$  and the text observation  $O_t$  at each time-step to select an action. As shown in Figure 2, the action selector consists of four main components: the *text encoder* and *graph encoder* convert text inputs and graph inputs, respectively, into hidden representations; a *representation aggregator* fuses the two representations using an attention mechanism; and a *scorer* ranks all candidate actions based on the aggregated representations.

- **Graph Encoder:** GATA’s belief graphs, which estimate the true game state, are multi-relational by design. Therefore, we use relational graph convolutional networks (R-GCNs) [32] to encode the belief graphs from the updater into vector representations. We also adapt the R-GCN model to use embeddings of the available relation labels, so that we can capture semantic correspondences among relations (e.g., `east_of` and `west_of` are reciprocal relations). We do so by learning a vector representation for each relation in the vocabulary that we condition on the word embeddings of the relation’s name. We concatenate the resulting vector with the standard node embeddings during R-GCN’s message passing phase. Our R-GCN implementation uses basis regularization [32] and highway connections [36] between layers for faster convergence. Details are given in Appendix A.1.
- **Text Encoder:** We adopt a transformer encoder [43] to convert text inputs from  $O_t$  and  $A_{t-1}$  into contextual vector representations. Details are provided in Appendix A.2.
- **Representation Aggregator:** To combine the text and graph representations, GATA uses a bi-directional attention-based aggregator [49, 33]. Attention from text to graph enables the agent to focus more on nodes that are currently observable, which are generally more relevant; attention from nodes to text enables the agent to focus more on tokens that appear in the graph, which are therefore connected with the player in certain relations. Details are provided in Appendix A.3.
- **Scorer:** The scorer consists of a self-attention layer cascaded with an MLP layer. First, the self-attention layer reinforces the dependency of every token-token pair and node-node pair in the aggregated representations. The resulting vectors are concatenated with the representations of action candidates  $C_t$  (from the text encoder), after which the MLP generates a single scalar for every action candidate as a score. Details are provided in Appendix A.4.

**Training the Action Selector:** We use Q-learning [45] to optimize the action selector on reward signals from the training games. Specifically, we use Double DQN [42] combined with multi-step learning [38] and prioritized experience replay [31]. To enable GATA to scale and generalize to multiple games, we adapt standard deep Q-Learning by sampling a new game from the set of training games to collect an episode. Consequently, the replay buffer contains transitions from episodes of different games. We provide further details on this training procedure in Appendix E.2.

### 3.4 Variants Using Ground-Truth Graphs

In GATA, the belief graph is learned entirely from text observations. However, the TextWorld API also provides access to the underlying graph states for games, in the format of discrete KGs. Thus, for comparison, we also consider two models that learn from or encode ground-truth graphs directly.

**GATA-GTP: Pre-training a *discrete* graph updater using ground-truth graphs.** We first consider a model that uses ground-truth graphs to pre-train the graph updater, in lieu of self-supervised methods. GATA-GTP uses ground-truth graphs from *FTWP* during pre-training, but infers belief graphs from the raw text during RL training of the action selector to compare fairly against GATA. Here, the belief graph  $\mathcal{G}_t$  is a discrete multi-relational graph. To pre-train a discrete graph updater, we adapt the

command generation approach proposed by Zelinka et al. [53]. We provide details of this approach in Appendix C.

**GATA-GTF: Training the action selector using ground-truth graphs.** To get a sense of the upper bound on performance we might obtain using a belief graph, we also train an agent that uses the full ground-truth graph  $\mathcal{G}^{\text{full}}$  during action selection. This agent requires no graph updater module; we simply feed the ground-truth graphs into the action selector (via the graph encoder). The use of ground-truth graphs allows GATA-GTF to escape the error cascades that may result from inferred belief graphs. Note also that the ground-truth graphs contain full state information, relaxing partial observability of the games. Consequently, we expect more effective reward optimization for GATA-GTF compared to other graph-based agents. GATA-GTF’s comparison with text-based agents is a sanity check for our hypothesis—that structured representations help learning general policies.

## 4 Experiments and Analysis

We conduct experiments on generated text-based games (Section 2) to answer two key questions:

**Q1:** Does the belief-graph approach aid GATA in achieving high rewards on unseen games after training? In particular, does GATA improve performance compared to SOTA text-based models?

**Q2:** How does GATA compare to models that have access to ground-truth graph representations?

### 4.1 Experimental Setup and Baselines

We divide the games into four subsets with one difficulty level per subset. Each subset contains 100 training, 20 validation, and 20 test games, which are sampled from a distribution determined by their difficulty level. To elaborate on the diversity of games: for easier games, the recipe might only require a single ingredient and the world is limited to a single location, whereas harder games might require an agent to navigate a map of 6 locations to collect and appropriately process up to three ingredients. We also test GATA’s transferability across difficulty levels by mixing the four difficulty levels to build level 5. We sample 25 games from each of the four difficulty levels to build a training set. We use all validation and test games from levels 1 to 4 for level 5 validation and test. In all experiments, we select the top-performing agent on validation sets and report its test scores; all validation and test games are unseen in the training set. Statistics of the games are shown in Table 1.

Table 1: Games statistics (averaged across all games within a difficulty level).

Level	Recipe Size	#Locations	Max Score	Need Cut	Need Cook	#Action Candidates	#Objects
1	1	1	4	✓	✗	11.5	17.1
2	1	1	5	✓	✓	11.8	17.5
3	1	9	3	✗	✗	7.2	34.1
4	3	6	11	✓	✓	28.4	33.4
5	Mixture of levels {1,2,3,4}						

As baselines, we use our implementation of LSTM-DQN [29] and LSTM-DRQN [50], both of which use only  $O_t$  as input. Note that LSTM-DRQN uses an RNN to enable an implicit memory (i.e., belief); it also uses an episodic counting bonus to encourage exploration [50]. This draws an interesting comparison with GATA, wherein the belief is extracted and updated dynamically, in the form of a graph. For fair comparison, we replace the LSTM-based text encoders with a transformer-based text encoder as in GATA. We denote those agents as Tr-DQN and Tr-DRQN respectively. We denote a Tr-DRQN equipped with the episodic counting bonus as Tr-DRQN+. These three text-based baselines are representative of the current top-performing neural agents on text-based games.

Additionally, we test the variants of GATA that have access to ground-truth graphs (as described in Section 3.4). Comparing with GATA, the GATA-GTP agent also maintains its belief graphs throughout the game; however, its graph updater is pre-trained on *FTWP* using ground-truth graphs—a stronger supervision signal. GATA-GTF, on the other hand, does not have a graph updater. It directly uses ground-truth graphs as input during game playing.



Table 2: Agents’ normalized **test** scores and averaged relative improvement (%  $\uparrow$ ) over Tr-DQN across difficulty levels. An agent m’s relative improvement over Tr-DQN is defined as  $(R_m - R_{\text{Tr-DQN}})/R_{\text{Tr-DQN}}$  where R is the score. All numbers are percentages.  $\blacklozenge$  represents ground-truth full graph;  $\clubsuit$  represents discrete  $\mathcal{G}_t$  generated by GATA-GTP;  $\spadesuit$  represents  $O_t$ .  $\star$  and  $\infty$  are continuous  $\mathcal{G}_t$  generated by GATA, when the graph updater is pre-trained with OG and COC tasks, respectively.

Difficulty Level	20 Training Games						100 Training Games						Avg.
	1	2	3	4	5	% $\uparrow$	1	2	3	4	5	% $\uparrow$	% $\uparrow$
Agent	Text-based Baselines												
Tr-DQN	66.2	26.0	16.7	18.2	<b>27.9</b>	—	62.5	32.0	38.3	17.7	34.6	—	—
Tr-DRQN	62.5	32.0	28.3	12.7	26.5	+10.3	58.8	31.0	36.7	21.4	27.4	-2.6	+3.9
Tr-DRQN+	65.0	30.0	35.0	11.8	18.3	+10.7	58.8	33.0	33.3	19.5	30.6	-3.4	+3.6
Input	GATA												
$\star$	70.0	20.0	20.0	18.6	26.3	-0.2	62.5	32.0	46.7	<b>27.7</b>	35.4	<b>+16.1</b>	+8.0
$\star\spadesuit$	66.2	<b>48.0</b>	26.7	15.5	26.3	+24.8	<b>66.2</b>	<b>36.0</b>	<b>58.3</b>	14.1	<b>45.0</b>	<b>+16.1</b>	+20.4
$\infty$	<b>73.8</b>	42.0	26.7	<b>20.9</b>	24.5	+27.1	62.5	30.0	51.7	23.6	36.0	+13.2	+20.2
$\infty\spadesuit$	68.8	33.0	<b>41.7</b>	17.7	27.0	<b>+34.9</b>	62.5	33.0	46.7	25.9	33.4	+13.6	<b>+24.2</b>
	GATA-GTP												
$\clubsuit$	56.2	26.0	40.0	17.3	17.7	+16.6	37.5	31.0	45.0	13.6	18.7	-18.9	-1.2
$\clubsuit\spadesuit$	65.0	32.0	41.7	12.3	23.5	+24.6	62.5	32.0	51.7	21.8	23.5	+5.2	+14.9
	GATA-GTF												
$\blacklozenge$	48.7	61.0	46.7	23.6	28.9	+64.2	95.0	95.0	70.0	37.3	52.8	+99.0	+81.6

### Q1: Performance of GATA compared to text-based baselines

In Table 2, we show the normalized test scores achieved by agents trained on either 20 or 100 games for each difficulty level. Equipped with belief graphs, GATA significantly outperforms all text-based baselines. The graph updater pre-trained on both of the self-supervised tasks (Section 3.2) leads to better performance than the baselines ( $\star$  and  $\infty$ ). We observe further improvements in GATA’s policies when the text observations ( $\spadesuit$ ) are also available. We believe the text observations guide GATA’s action scorer to focus on currently observable objects through the bi-attention mechanism. The attention may further help GATA to counteract accumulated errors from the belief graphs. In addition, we observe that Tr-DRQN and Tr-DRQN+ outperform Tr-DQN, with 3.9% and 3.6% relative improvement (%  $\uparrow$ ). This suggests the implicit memory of the recurrent components improves performance. We also observe GATA substantially outperforms Tr-DQN when trained on 100 games, whereas the DRQN agents struggle to optimize rewards on the larger training sets.

### Q2: Performance of GATA compared to models with access to the ground-truth graph

Table 2 also reports test performance for GATA-GTP ( $\clubsuit$ ) and GATA-GTF ( $\blacklozenge$ ). Consistent with GATA, we find GATA-GTP also performs better when given text observations ( $\spadesuit$ ) as additional input to the action scorer. Although GATA-GTP outperforms Tr-DQN by 14.9% when text observations are available, its overall performance is still substantially poorer than GATA. Although the graph updater in GATA-GTP is trained with ground-truth graphs, we believe the discrete belief graphs and the discrete operations for updating them (Appendix C.1) make this approach vulnerable to an accumulation of errors over game steps, as well as errors introduced by the discrete nature of the predictions (e.g., round-off error). In contrast, we suspect that the continuous belief graph and the learned graph operation function (Eqn. 2) are easier to train and recover more gracefully from errors.

Meanwhile, GATA-GTF, which uses ground-truth graphs  $\mathcal{G}^{\text{full}}$  during training and testing, obtains significantly higher scores than does GATA and all other baselines. Because  $\mathcal{G}^{\text{full}}$  turns the game environment into a fully observable MDP and encodes accurate state information with no error accumulation, GATA-GTF represents the performance upper-bound of all the  $\mathcal{G}_t$ -based baselines. The scores achieved by GATA-GTF reinforce our intuition that belief graphs improve text-based game

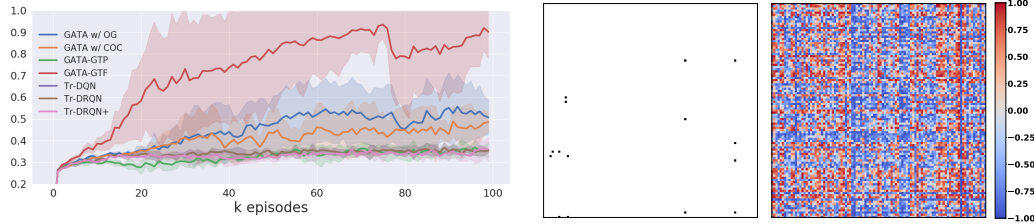


Figure 3: **Left:** Training curves on 20 level 2 games (averaged over 3 seeds). **Right:** Density comparison between a ground-truth graph (binary) and a belief graph  $\mathcal{G}$  generated by the COC pre-training procedure. Both matrices are slices of adjacency tensors corresponding to the `is` relation.

agents. At the same time, the performance gap between GATA and GATA-GTF invites investigation into better ways to learn accurate graph representations of text.

### Additional Results

We also show the agents’ training curves and examples of the belief graphs  $\mathcal{G}$  generated by GATA. Figure 3 (**Left**) shows an example of all agents’ training curves. We observe consistent trends with the testing results of Table 2 — GATA outperforms the text-based baselines and GATA-GTP, but a significant gap exists between GATA and GATA-GTF (which uses ground-truth graphs as input to the action scorer). Figure 3 (**Right**) highlights the sparsity of a ground-truth graph compared to that of a belief graph  $\mathcal{G}$ . Since generation of  $\mathcal{G}$  is unsupervised by any ground-truth graphs, we do not expect  $\mathcal{G}$  to be interpretable nor sparse. Further, since the self-supervised models learn belief graphs directly from text, some of the learned features may correspond to the underlying grammar or other features useful for the self-supervised tasks, rather than only being indicative of relationships between objects. However, we show  $\mathcal{G}$  encodes useful information for a relation prediction probing task in Appendix D.5.

Given space limitations, we only report a representative selection of our results in this section. Appendix D provides an exhaustive set of results including training curves, training scores, and test scores for all experimental settings introduced in this work. We also provide a detailed qualitative analysis including hi-res visualizations of the belief graphs. We encourage readers to refer to it.

## 5 Related Work

**Dynamic graph extraction:** Numerous recent works have focused on constructing graphs to encode structured representations of raw data, for various tasks. Kipf et al. [23] propose contrastive methods to learn latent structured world models (C-SWMs) as state representations for vision-based environments. Their work, however, does not focus on learning policies to play games or to generalize across varying environments. Das et al. [10] leverage a machine reading comprehension mechanism to query for entities and states in short text passages and use a dynamic graph structure to track changing entity states. Fan et al. [12] propose to encode graph representations by linearizing the graph as an input sequence in NLP tasks. Johnson [21] construct graphs from text data using gated graph transformer neural networks. Yang et al. [46] learn transferable latent relational graphs from raw data in a self-supervised manner. Compared to the existing literature, our work aims to infer multi-relational KGs dynamically from partial text observations of the state and subsequently use these graphs to inform general policies. Concurrently, Srinivas et al. [35] propose to learn state representations with contrastive learning methods to facilitate RL training. However, they focus on vision-based environments and they do not investigate generalization.

More generally, we want to note that compared to traditional knowledge base construction (KBC) works, our approach is more related to the direction of neural relational inference [22]. In particular, we seek to generate task-specific graphs, which tend to be dynamic, contextual and relatively small, whereas traditional KBC focus on generating large, static graphs.

**Playing Text-based Games:** Recent years have seen a host of work on playing text-based games. Various deep learning agents have been explored [29, 17, 14, 51, 20, 3, 52, 47]. Fulda et al. [13] use pre-trained embeddings to reduce the action space. Zahavy et al. [51], Seurin et al. [34], and



Jain et al. [20] explicitly condition an agent’s decisions on game feedback. Most of this literature trains and tests on a single game without considering generalization. Urbanek et al. [40] use memory networks and ranking systems to tackle adventure-themed dialog tasks. Yuan et al. [50] propose a count-based memory to explore and generalize on simple unseen text-based games. Madotto et al. [26] use GoExplore [11] with imitation learning to generalize. Adolphs and Hofmann [1] and Yin and May [48] also investigate the multi-game setting. These methods rely either on reward shaping by heuristics, imitation learning, or rule-based features as inputs. We aim to minimize hand-crafting, so our action selector is optimized only using raw rewards from games while other components of our model are pre-trained on related data. Recently, Ammanabrolu and Riedl [4], Ammanabrolu and Hausknecht [3], Yin and May [48] leverage graph structure by using rule-based, untrained mechanisms to construct KGs to play text-based games.

## 6 Conclusion

In this work, we investigate how an RL agent can play and generalize within a distribution of text-based games using graph-structured representations inferred from text. We introduce GATA, a novel neural agent that infers and updates latent belief graphs as it plays text-based games. We use a combination of RL and self-supervised learning to teach the agent to encode essential dynamics of the environment in its belief graphs. We show that GATA achieves good test performance, outperforming a set of strong baselines including agents pre-trained with ground-truth graphs. This evinces the effectiveness of generating graph-structured representations for text-based games.

## 7 Broader Impact

Our work’s immediate aim—improved performance on text-based games—might have limited consequences for society; however, taking a broader view of our work and where we’d like to take it forces us to consider several social and ethical concerns. We use text-based games as a proxy to model and study the interaction of machines with the human world, through language. Any system that interacts with the human world impacts it. As mentioned previously, an example of language-mediated, human-machine interaction is online customer service systems.

- In these systems, especially in products related to critical needs like healthcare, providing inaccurate information could result in serious harm to users. Likewise, failing to communicate clearly, sensibly, or convincingly might also cause harm. It could waste users’ precious time and diminish their trust.
- The responses generated by such systems must be inclusive and free of bias. They must not cause harm by the act of communication itself, nor by making decisions that disenfranchise certain user groups. Unfortunately, many data-driven, free-form language generation systems currently exhibit bias and/or produce problematic outputs.
- Users’ privacy is also a concern in this setting. Mechanisms must be put in place to protect it. Agents that interact with humans almost invariably train on human data; their function requires that they solicit, store, and act upon sensitive user information (especially in the healthcare scenario envisioned above). Therefore, privacy protections must be implemented throughout the agent development cycle, including data collection, training, and deployment.
- Tasks that require human interaction through language are currently performed by people. As a result, advances in language-based agents may eventually displace or disrupt human jobs. This is a clear negative impact.

Even more broadly, any systems that generate convincing natural language could be used to spread misinformation.

Our work is immediately aimed at improving the performance of RL agents in text-based games, in which agents must understand and act in the world through language. Our hope is that this work, by introducing graph-structured representations, endows language-based agents with greater accuracy and clarity, and the ability to make better decisions. Similarly, we expect that graph-structured representations could be used to constrain agent decisions and outputs, for improved safety. Finally, we believe that structured representations can improve neural agents’ interpretability to researchers and users. This is an important future direction that can contribute to accountability and transparency

in AI. As we have outlined, however, this and future work must be undertaken with awareness of its hazards.

## 8 Acknowledgements

We thank Alessandro Sordani and Devon Hjelm for the helpful discussions about the probing task. We also thank David Krueger, Devendra Singh Sachan, Harm van Seijen, Harshita Sahijwani, Jacob Miller, Koustuv Sinha, Loren Lugosch, Meng Qu, Travis LaCroix, and the anonymous ICML 2020 and NeurIPS 2020 reviewers and ACs for their insightful comments on an earlier draft of this work. The work was funded in part by an academic grant from Microsoft Research, an NSERC Discovery Grant RGPIN-2019-05123, an IVADO Fundamental Research Project Grant PRF-2019-3583139727, as well as Canada CIFAR Chairs in AI, held by Prof. Hamilton, Prof. Poupart and Prof. Tang.

## References

- [1] Adolphs, L. and Hofmann, T. (2019). Ledeeepchef: Deep reinforcement learning agent for families of text-based games. *CoRR*, abs/1909.01646.
- [2] Alain, G. and Bengio, Y. (2017). Understanding intermediate layers using linear classifier probes. *ArXiv*, abs/1610.01644.
- [3] Ammanabrolu, P. and Hausknecht, M. (2020). Graph constrained reinforcement learning for natural language action spaces. In *International Conference on Learning Representations*.
- [4] Ammanabrolu, P. and Riedl, M. (2019). Playing text-adventure games with graph-based deep reinforcement learning. In *Proceedings of the 2019 Conference of the North American Chapter of the Association for Computational Linguistics: Human Language Technologies, Volume 1 (Long and Short Papers)*, pages 3557–3565, Minneapolis, Minnesota. Association for Computational Linguistics.
- [5] Atkinson, T., Baier, H., Copplestone, T., Devlin, S., and Swan, J. (2018). The text-based adventure ai competition. *IEEE Transactions on Games*, 11:260–266.
- [6] Ba, L. J., Kiros, J. R., and Hinton, G. E. (2016). Layer normalization. *CoRR*, abs/1607.06450.
- [7] Bachman, P., Hjelm, R. D., and Buchwalter, W. (2019). Learning representations by maximizing mutual information across views. In *Advances in Neural Information Processing Systems*, pages 15509–15519.
- [8] Cho, K., van Merriënboer, B., Gulcehre, C., Bahdanau, D., Bougares, F., Schwenk, H., and Bengio, Y. (2014). Learning phrase representations using RNN encoder–decoder for statistical machine translation. In *Proceedings of the 2014 Conference on Empirical Methods in Natural Language Processing (EMNLP)*, pages 1724–1734, Doha, Qatar. Association for Computational Linguistics.
- [9] Côté, M.-A., Kádár, A., Yuan, X., Kybartas, B., Barnes, T., Fine, E., Moore, J., Tao, R. Y., Hausknecht, M., Asri, L. E., Adada, M., Tay, W., and Trischler, A. (2018). Textworld: A learning environment for text-based games. *CoRR*, abs/1806.11532.
- [10] Das, R., Munkhdalai, T., Yuan, X., Trischler, A., and McCallum, A. (2019). Building dynamic knowledge graphs from text using machine reading comprehension. In *International Conference on Learning Representations*.
- [11] Ecoffet, A., Huizinga, J., Lehman, J., Stanley, K. O., and Clune, J. (2019). Go-explore: a new approach for hard-exploration problems. *ArXiv*, abs/1901.10995.
- [12] Fan, A., Gardent, C., Braud, C., and Bordes, A. (2019). Using local knowledge graph construction to scale Seq2Seq models to multi-document inputs. In *Proceedings of the 2019 Conference on Empirical Methods in Natural Language Processing and the 9th International Joint Conference on Natural Language Processing (EMNLP-IJCNLP)*, pages 4186–4196, Hong Kong, China. Association for Computational Linguistics.

- [13] Fulda, N., Ricks, D., Murdoch, B., and Wingate, D. (2017). What can you do with a rock? affordance extraction via word embeddings. In *Proceedings of the Twenty-Sixth International Joint Conference on Artificial Intelligence, IJCAI-17*, pages 1039–1045.
- [14] Hausknecht, M., Ammanabrolu, P., Marc-Alexandre, C., and Yuan, X. (2020). Interactive fiction games: A colossal adventure. In *Thirty-Fourth AAAI Conference on Artificial Intelligence*.
- [15] Hausknecht, M. and Stone, P. (2015). Deep recurrent q-learning for partially observable mdps. In *AAAI Fall Symposium on Sequential Decision Making for Intelligent Agents (AAAI-SDMIA15)*.
- [16] Hausknecht, M. J., Loynd, R., Yang, G., Swaminathan, A., and Williams, J. D. (2019). Nail: A general interactive fiction agent. *CoRR*, abs/1902.04259.
- [17] He, J., Chen, J., He, X., Gao, J., Li, L., Deng, L., and Ostendorf, M. (2016). Deep reinforcement learning with a natural language action space. In *Proceedings of the 54th Annual Meeting of the Association for Computational Linguistics (Volume 1: Long Papers)*, pages 1621–1630, Berlin, Germany. Association for Computational Linguistics.
- [18] Hessel, M., Modayil, J., Van Hasselt, H., Schaul, T., Ostrovski, G., Dabney, W., Horgan, D., Piot, B., Azar, M., and Silver, D. (2018). Rainbow: Combining improvements in deep reinforcement learning. In *Thirty-Second AAAI Conference on Artificial Intelligence*.
- [19] Hjelm, D., Fedorov, A., Lavoie-Marchildon, S., Grewal, K., Bachman, P., Trischler, A., and Bengio, Y. (2019). Learning deep representations by mutual information estimation and maximization. In *ICLR 2019*. ICLR.
- [20] Jain, V., Fedus, W., Larochelle, H., Precup, D., and Bellemare, M. G. (2020). Algorithmic improvements for deep reinforcement learning applied to interactive fiction. In *Thirty-Fourth AAAI Conference on Artificial Intelligence*.
- [21] Johnson, D. D. (2017). Learning graphical state transitions. In *International Conference on Learning Representations (ICLR)*.
- [22] Kipf, T., Fetaya, E., Wang, K.-C., Welling, M., and Zemel, R. (2018). Neural relational inference for interacting systems. *arXiv preprint arXiv:1802.04687*.
- [23] Kipf, T., van der Pol, E., and Welling, M. (2020). Contrastive learning of structured world models. In *International Conference on Learning Representations*.
- [24] Lima, P. (2019). First textworld challenge - first place solution.
- [25] Liu, L., Jiang, H., He, P., Chen, W., Liu, X., Gao, J., and Han, J. (2020). On the variance of the adaptive learning rate and beyond. In *Proceedings of the Eighth International Conference on Learning Representations (ICLR 2020)*.
- [26] Madotto, A., Namazifar, M., Huizinga, J., Molino, P., Ecoffet, A., Zheng, H., Papangelis, A., Yu, D., Khatri, C., and Tur, G. (2020). Exploration based language learning for text-based games.
- [27] Meng, R., Yuan, X., Wang, T., Brusilovsky, P., Trischler, A., and He, D. (2019). Does order matter? an empirical study on generating multiple keyphrases as a sequence. *CoRR*.
- [28] Mikolov, T., Grave, E., Bojanowski, P., Puhersch, C., and Joulin, A. (2018). Advances in pre-training distributed word representations. In *Proceedings of the International Conference on Language Resources and Evaluation (LREC 2018)*.
- [29] Narasimhan, K., Kulkarni, T., and Barzilay, R. (2015). Language understanding for text-based games using deep reinforcement learning. In *Proceedings of the 2015 Conference on Empirical Methods in Natural Language Processing*, pages 1–11, Lisbon, Portugal. Association for Computational Linguistics.
- [30] Paszke, A., Gross, S., Chintala, S., Chanan, G., Yang, E., DeVito, Z., Lin, Z., Desmaison, A., Antiga, L., and Lerer, A. (2017). Automatic differentiation in pytorch. In *NIPS-W*.
- [31] Schaul, T., Quan, J., Antonoglou, I., and Silver, D. (2016). Prioritized experience replay. In *International Conference on Learning Representations*, Puerto Rico.

- [32] Schlichtkrull, M., Kipf, T. N., Bloem, P., Van Den Berg, R., Titov, I., and Welling, M. (2018). Modeling relational data with graph convolutional networks. In *European Semantic Web Conference*, pages 593–607. Springer.
- [33] Seo, M. J., Kembhavi, A., Farhadi, A., and Hajishirzi, H. (2017). Bidirectional attention flow for machine comprehension. In *5th International Conference on Learning Representations, ICLR 2017, Toulon, France, April 24-26, 2017, Conference Track Proceedings*. OpenReview.net.
- [34] Seurin, M., Preux, P., and Pietquin, O. (2019). “i’m sorry dave, i’m afraid i can’t do that” deep q-learning from forbidden action. *CoRR*, abs/1910.02078.
- [35] Srinivas, A., Laskin, M., and Abbeel, P. (2020). Curl: Contrastive unsupervised representations for reinforcement learning. *arXiv preprint arXiv:2004.04136*.
- [36] Srivastava, R. K., Greff, K., and Schmidhuber, J. (2015). Highway networks. *CoRR*, abs/1505.00387.
- [37] Sutton, R. (2019). *The Bitter Lesson*.
- [38] Sutton, R. S. (1988). Learning to predict by the methods of temporal differences. *Machine Learning*, 3(1):9–44.
- [39] Trischler, A., Côté, M.-A., and Lima, P. (2019). *First TextWorld Problems, the competition: Using text-based games to advance capabilities of AI agents*.
- [40] Urbanek, J., Fan, A., Karamcheti, S., Jain, S., Humeau, S., Dinan, E., Rocktäschel, T., Kiela, D., Szlam, A., and Weston, J. (2019). Learning to speak and act in a fantasy text adventure game. *CoRR*, abs/1903.03094.
- [41] van den Oord, A., Li, Y., and Vinyals, O. (2018). Representation learning with contrastive predictive coding. *CoRR*, abs/1807.03748.
- [42] van Hasselt, H., Guez, A., and Silver, D. (2015). Deep reinforcement learning with double q-learning. In *AAAI*.
- [43] Vaswani, A., Shazeer, N., Parmar, N., Uszkoreit, J., Jones, L., Gomez, A. N., Kaiser, L. u., and Polosukhin, I. (2017). Attention is all you need. In Guyon, I., Luxburg, U. V., Bengio, S., Wallach, H., Fergus, R., Vishwanathan, S., and Garnett, R., editors, *Advances in Neural Information Processing Systems 30*, pages 5998–6008. Curran Associates, Inc.
- [44] Veličković, P., Fedus, W., Hamilton, W. L., Liò, P., Bengio, Y., and Hjelm, R. D. (2019). Deep Graph Infomax. In *International Conference on Learning Representations*.
- [45] Watkins, C. J. C. H. and Dayan, P. (1992). Q-learning. *Machine Learning*, 8(3):279–292.
- [46] Yang, Z., Zhao, J., Dhingra, B., He, K., Cohen, W. W., Salakhutdinov, R. R., and LeCun, Y. (2018). Glomo: Unsupervised learning of transferable relational graphs. In Bengio, S., Wallach, H., Larochelle, H., Grauman, K., Cesa-Bianchi, N., and Garnett, R., editors, *Advances in Neural Information Processing Systems 31*, pages 8950–8961. Curran Associates, Inc.
- [47] Yin, X. and May, J. (2019a). Comprehensible context-driven text game playing. In *2019 IEEE Conference on Games (CoG)*, pages 1–8. IEEE.
- [48] Yin, X. and May, J. (2019b). Learn how to cook a new recipe in a new house: Using map familiarization, curriculum learning, and bandit feedback to learn families of text-based adventure games. *CoRR*, abs/1908.04777.
- [49] Yu, A. W., Dohan, D., Luong, M., Zhao, R., Chen, K., Norouzi, M., and Le, Q. V. (2018). Qanet: Combining local convolution with global self-attention for reading comprehension. In *International Conference on Learning Representations*.
- [50] Yuan, X., Côté, M.-A., Sordoni, A., Larochelle, R., Combes, R. T. d., Hausknecht, M., and Trischler, A. (2018). Counting to explore and generalize in text-based games. *arXiv preprint arXiv:1806.11525*.

- [51] Zahavy, T., Haroush, M., Merlis, N., Mankowitz, D. J., and Mannor, S. (2018). Learn what not to learn: Action elimination with deep reinforcement learning. In *Advances in Neural Information Processing Systems*, pages 3562–3573.
- [52] Zelinka, M. (2018). Baselines for reinforcement learning in text games. *2018 IEEE 30th International Conference on Tools with Artificial Intelligence (ICTAI)*, pages 320–327.
- [53] Zelinka, M., Yuan, X., Cote, M.-A., Laroche, R., and Trischler, A. (2019). Building dynamic knowledge graphs from text-based games. *arXiv preprint arXiv:1910.09532*.

## Contents in Appendices:

- In Appendix A, we describe each of the components in GATA in detail.
- In Appendix B, we provide detailed information on how we pre-train GATA’s graph updater with the two proposed methods (i.e., OG and COC).
- In Appendix C, we provide detailed information on GATA-GTP, the discrete version of GATA. Since the action scorer module is the same as in GATA, this appendix elaborates on how a discrete graph updater works and how to pre-train the discrete graph updater.
- In Appendix D, we provide additional results and discussions. This includes training curves, training scores, testing scores, and high-res examples of the belief graphs learned by GATA. We provide a set of probing experiments to show that the belief graphs learned by GATA can capture useful information for relation classification tasks. We also provide qualitative analysis on GATA’s OG task, which also suggests the belief graphs contain useful information for reconstructing the text observation  $O_t$ .
- In Appendix E, we provide implementation details for all our experiments.
- In Appendix F, we show examples of graphs in TextWorld games.

## A Details of GATA

### Notations

In this section, we use  $O_t$  to denote text observation at game step  $t$ ,  $C_t$  to denote a list of action candidate provided by a game, and  $\mathcal{G}_t$  to denote a belief graph that represents GATA’s belief to the state.

We use  $L$  to refer to a linear transformation and  $L^f$  means it is followed by a non-linear activation function  $f$ . Brackets  $[\cdot; \cdot]$  denote vector concatenation. Overall structure of GATA is shown in Figure 2.

### A.1 Graph Encoder

As briefly mentioned in Section 3.3, GATA utilizes a graph encoder which is based on R-GCN [32].

To better leverage information from relation labels, when computing each node’s representation, we also condition it on a relation representation  $E$ :

$$\tilde{h}_i = \sigma \left( \sum_{r \in \mathcal{R}} \sum_{j \in \mathcal{N}_i^r} W_r^l [h_j^l; E_r] + W_0^l [h_i^l; E_r] \right), \quad (5)$$

in which,  $l$  denotes the  $l$ -th layer of the R-GCN,  $\mathcal{N}_i^r$  denotes the set of neighbor indices of node  $i$  under relation  $r \in \mathcal{R}$ ,  $\mathcal{R}$  indicates the set of different relations,  $W_r^l$  and  $W_0^l$  are trainable parameters. Since we use continuous graphs,  $\mathcal{N}_i^r$  includes all nodes (including node  $i$  itself). To stabilize the model and preventing from the potential explosion introduced by stacking R-GCNs with continuous graphs, we use Sigmoid function as  $\sigma$  (in contrast with the commonly used ReLU function).

As the initial input  $h^0$  to the graph encoder, we concatenate a node embedding vector and the averaged word embeddings of node names. Similarly, for each relation  $r$ ,  $E_r$  is the concatenation of a relation embedding vector and the averaged word embeddings of  $r$ ’s label. Both node embedding and relation embedding vectors are randomly initialized and trainable.

To further help our graph encoder to learn with multiple layers of R-GCN, we add highway connections [36] between layers:

$$\begin{aligned} g &= L^{\text{sigmoid}}(\tilde{h}_i), \\ h_i^{l+1} &= g \odot \tilde{h}_i + (1 - g) \odot h_i^l, \end{aligned} \quad (6)$$

where  $\odot$  indicates element-wise multiplication.

We use a 6-layer graph encoder, with a hidden size  $H$  of 64 in each layer. The node embedding size is 100, relation embedding size is 32. The number of bases we use is 3.



## A.2 Text Encoder

We use a transformer-based text encoder, which consists of a word embedding layer and a transformer block [43]. Specifically, word embeddings are initialized by the 300-dimensional fastText [28] word vectors trained on Common Crawl (600B tokens) and kept fixed during training in all settings.

The transformer block consists of a stack of 5 convolutional layers, a self-attention layer, and a 2-layer MLP with a ReLU non-linear activation function in between. In the block, each convolutional layer has 64 filters, each kernel’s size is 5. In the self-attention layer, we use a block hidden size  $H$  of 64, as well as a single head attention mechanism. Layernorm [6] is applied after each component inside the block. Following standard transformer training, we add positional encodings into each block’s input.

We use the same text encoder to process text observation  $O_t$  and the action candidate list  $C_t$ . The resulting representations are  $h_{O_t} \in \mathbb{R}^{L_{O_t} \times H}$  and  $h_{C_t} \in \mathbb{R}^{N_{C_t} \times L_{C_t} \times H}$ , where  $L_{O_t}$  is the number of tokens in  $O_t$ ,  $N_{C_t}$  denotes the number of action candidates provided,  $L_{C_t}$  denotes the maximum number of tokens in  $C_t$ , and  $H = 64$  is the hidden size.

## A.3 Representation Aggregator

The representation aggregator aims to combine the text observation representations and graph representations together. Therefore this module is activated only when both the text observation  $O_t$  and the graph input  $\mathcal{G}_t$  are provided. In cases where either of them is absent, for instance, when training the agent with only  $\mathcal{G}^{\text{belief}}$  as input, the aggregator will be deactivated and the graph representation will be directly fed into the scorer.

For simplicity, we omit the subscript  $t$  denoting game step in this subsection. At any game step, the graph encoder processes graph input  $\mathcal{G}$ , and generates the graph representation  $h_{\mathcal{G}} \in \mathbb{R}^{N_{\mathcal{G}} \times H}$ . The text encoder processes text observation  $O$  to generate text representation  $h_O \in \mathbb{R}^{L_O \times H}$ .  $N_{\mathcal{G}}$  denotes the number of nodes in the graph  $\mathcal{G}$ ,  $L_O$  denotes the number of tokens in  $O$ .

We adopt a standard representation aggregation method from question answering literature [49] to combine the two representations using attention mechanism.

Specifically, the aggregator first uses an MLP to convert both  $h_{\mathcal{G}}$  and  $h_O$  into the same space, the resulting tensors are denoted as  $h'_{\mathcal{G}} \in \mathbb{R}^{N_{\mathcal{G}} \times H}$  and  $h'_O \in \mathbb{R}^{L_O \times H}$ . Then, a trilinear similarity function [33] is used to compute the similarities between each token in  $h'_O$  with each node in  $h'_{\mathcal{G}}$ . The similarity between  $i$ th token in  $h'_O$  and  $j$ th node in  $h'_{\mathcal{G}}$  is thus computed by:

$$\text{Sim}(i, j) = W(h'_{O_i}, h'_{\mathcal{G}_j}, h'_{O_i} \odot h'_{\mathcal{G}_j}), \quad (7)$$

where  $W$  is trainable parameters in the trilinear function. By applying the above computation for each pair of  $h'_O$  and  $h'_{\mathcal{G}}$ , a similarity matrix  $S \in \mathbb{R}^{L_O \times N_{\mathcal{G}}}$  is resulted.

Softmax of the similarity matrix  $S$  along both dimensions (number of nodes  $N_{\mathcal{G}}$  and number of tokens  $L_O$ ) are computed, producing  $S_{\mathcal{G}}$  and  $S_O$ . The information contained in the two representations are then aggregated by:

$$\begin{aligned} h_{O\mathcal{G}} &= [h'_O; P; h'_O \odot P; h'_O \odot Q], \\ P &= S_{\mathcal{G}} h_{\mathcal{G}}^{\top}, \\ Q &= S_{\mathcal{G}} S_O^{\top} h_O^{\top}, \end{aligned} \quad (8)$$

where  $h_{O\mathcal{G}} \in \mathbb{R}^{L_O \times 4H}$  is the aggregated observation representation, each token in text is represented by the weighted sum of graph representations. Similarly, the aggregated graph representation  $h_{\mathcal{G}O} \in \mathbb{R}^{N_{\mathcal{G}} \times 4H}$  can also be obtained, where each node in the graph is represented by the weighted sum of text representations. Finally, a linear transformation projects the two aggregated representations to a space with size  $H$  of 64:

$$\begin{aligned} h_{\mathcal{G}O} &= L(h_{\mathcal{G}O}), \\ h_{O\mathcal{G}} &= L(h_{O\mathcal{G}}). \end{aligned} \quad (9)$$

#### A.4 Scorer

The scorer consists of a self-attention layer, a masked mean pooling layer, and a two-layer MLP. As shown in Figure 2 and described above, the input to the scorer is the action candidate representation  $h_{C_t}$ , and one of the following game state representation:

$$s_t = \begin{cases} h_{\mathcal{G}_t} & \text{if only graph input is available,} \\ h_{O_t} & \text{if only text observation is available, this degrades GATA to a Tr-DQN,} \\ h_{\mathcal{G}_{O_t}}, h_{O_{\mathcal{G}_t}} & \text{if both are available.} \end{cases}$$

First, a self-attention is applied to the game state representation  $s_t$ , producing  $\hat{s}_t$ . If  $s_t$  includes graph representations, this self-attention mechanism will reinforce the connection between each node and its related nodes. Similarly, if  $s_t$  includes text representation, the self-attention mechanism strengthens the connection between each token and other related tokens. Further, masked mean pooling is applied to the self-attended state representation  $\hat{s}_t$  and the action candidate representation  $h_{C_t}$ , this results in a state representation vector and a list of action candidate representation vectors. We then concatenate the resulting vectors and feed them into a 2-layer MLP with a ReLU non-linear activation function in between. The second MLP layer has an output dimension of 1, after squeezing the last dimension, the resulting vector is of size  $N_{C_t}$ , which is the number of action candidates provided at game step  $t$ . We use this vector as the score of each action candidate.

#### A.5 The $f_{\Delta}$ Function

As mentioned in Eqn. 2,  $f_{\Delta}$  is an aggregator that combines information in  $\mathcal{G}_{t-1}$ ,  $A_{t-1}$ , and  $O_t$  to generate the graph difference  $\Delta g_t$ .

In specific,  $f_{\Delta}$  uses the same architecture as the representation aggregator described in Appendix A.3. Denoting the aggregator as a function Aggr:

$$h_{PQ}, h_{QP} = \text{Aggr}(h_P, h_Q), \quad (10)$$

$f_{\Delta}$  takes text observation representations  $h_{O_t} \in \mathbb{R}^{L_{O_t} \times H}$ , belief graph representations  $h_{\mathcal{G}_{t-1}} \in \mathbb{R}^{N_{\mathcal{G}} \times H}$ , and action representations  $h_{A_{t-1}} \in \mathbb{R}^{L_{A_{t-1}} \times H}$  as input.  $L_{O_t}$  and  $L_{A_{t-1}}$  are the number of tokens in  $O_t$  and  $A_{t-1}$ , respectively;  $N_{\mathcal{G}}$  is the number of nodes in the graph;  $H$  is hidden size of the input representations.

We first aggregate  $h_{O_t}$  with  $h_{\mathcal{G}_{t-1}}$ , then similarly  $h_{A_{t-1}}$  with  $h_{\mathcal{G}_{t-1}}$ :

$$\begin{aligned} h_{OG}, h_{GO} &= \text{Aggr}(h_{O_t}, h_{\mathcal{G}_{t-1}}), \\ h_{AG}, h_{GA} &= \text{Aggr}(h_{A_{t-1}}, h_{\mathcal{G}_{t-1}}). \end{aligned} \quad (11)$$

The output of  $f_{\Delta}$  is:

$$\Delta g_t = [h_{OG}^{\bar{X}}; h_{GO}^{\bar{X}}; h_{AG}^{\bar{X}}; h_{GA}^{\bar{X}}], \quad (12)$$

where  $\bar{X}$  is the masked mean of  $X$  on the first dimension. The resulting concatenated vector  $\Delta g_t$  has the size of  $\mathbb{R}^{4H}$ .

#### A.6 The $f_d$ Function

$f_d$  is a decoder that maps a hidden graph representation  $h_t \in \mathbb{R}^H$  (generated by the RNN) into a continuous adjacency tensor  $\mathcal{G} \in [-1, 1]^{2\mathcal{R} \times \mathcal{N} \times \mathcal{N}}$ .

Specifically,  $f_d$  consists of a 2-layer MLP:

$$\begin{aligned} h_1 &= L_1^{\text{ReLU}}(h_t), \\ h_2 &= L_2^{\text{tanh}}(h_1). \end{aligned} \quad (13)$$

In which,  $h_1 \in \mathbb{R}^H$ ,  $h_2 \in [-1, 1]^{2\mathcal{R} \times \mathcal{N} \times \mathcal{N}}$ . To better facilitate the message passing process of R-GCNs used in GATA's graph encoder, we explicitly use the transposed  $h_2$  to represent the inversed relations in the belief graph. Thus, we have  $\mathcal{G}$  defined as:

$$\mathcal{G} = [h_2; h_2^T]. \quad (14)$$

The transpose is performed on the last two dimensions (both of size  $\mathcal{N}$ ), the concatenation is performed on the dimension of relations.

The tanh activation function on top of the second layer of the MLP restricts the range of our belief graph  $\mathcal{G}$  within  $[-1, 1]$ . Empirically we find it helpful to keep the input of the multi-layer graph neural networks (the R-GCN graph encoder) in this range.

## B Details of Pre-training Graph Updater for GATA

As briefly described in Section 3.2, we design two self-supervised tasks to pre-train the graph updater module of GATA. As training data, we gather a collection of transitions from the *FTWP* dataset. Here, we denote a transition as a 3-tuple  $(O_{t-1}, A_{t-1}, O_t)$ . Specifically, given text observation  $O_{t-1}$ , an action  $A_{t-1}$  is issued; this leads to a new game state and  $O_t$  is returned from the game engine. Since the graph updater is recurrent (we use an RNN as its graph operation function), the set of transitions are stored in the order they are collected.

### B.1 Observation Generation (OG)

As shown in Figure 4, given a transition  $(O_{t-1}, A_{t-1}, O_t)$ , we use the belief graph  $\mathcal{G}_t$  and  $A_{t-1}$  to reconstruct  $O_t$ .  $\mathcal{G}_t$  is generated by the graph updater, conditioned on the recurrent information  $h_{t-1}$  carried over from previous data point in the transition sequence.

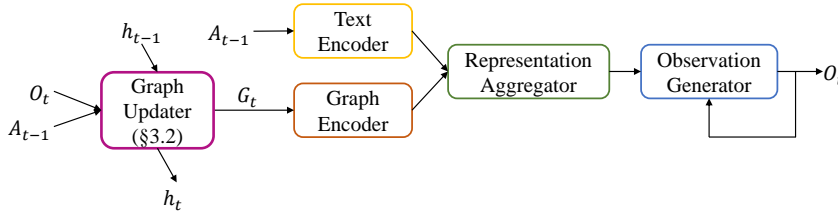


Figure 4: Observation generation model.

#### B.1.1 Observation Generator Layer

The observation generator is a transformer-based decoder. It consists of a word embedding layer, a transformer block, and a projection layer.

Similar to the text encoder, the embedding layer is frozen after initializing with the pre-trained fastText [28] word embeddings. Inside the transformer block, there is one self attention layer, two attention layers and a 3-layer MLP with ReLU non-linear activation functions in between. Taking word embedding vectors and the two aggregated representations produced by the representation aggregator as input, the self-attention layer first generates a contextual encoding vectors for the words. These vectors are then fed into the two attention layers to compute attention with graph representations and text observation representations respectively. The two resulting vectors are thus concatenated, and they are fed into the 3-layer MLP. The block hidden size of this transformer is  $H = 64$ .

Finally, the output of the transformer block is fed into the projection layer, which is a linear transformation with output size same as the vocabulary size. The resulting logits are then normalized by a softmax to generate a probability distribution over all words in vocabulary.

Following common practice, we also use a mask to prevent the decoder transformer to access “future” information during training.

### B.2 Contrastive Observation Classification (COC)

The contrastive observation classification task shares the same goal of ensuring the generated belief graph  $\mathcal{G}_t$  encodes the necessary information describing the environment state at step  $t$ . However, instead of generating  $O_t$  from  $\mathcal{G}_t$ , it requires a model to differentiate the real  $O_t$  from some  $\tilde{O}_t$  that are randomly sampled from other data points. In this task, the belief graph does not need to encode

the syntactical information as in the observation generation task, rather, a model can use its full capacity to learn the semantic information of the current environmental state.

We illustrate our contrastive observation classification model in Figure 5. This model shares most components with the previously introduced observation generation model, except replacing the observation generator module by a discriminator.

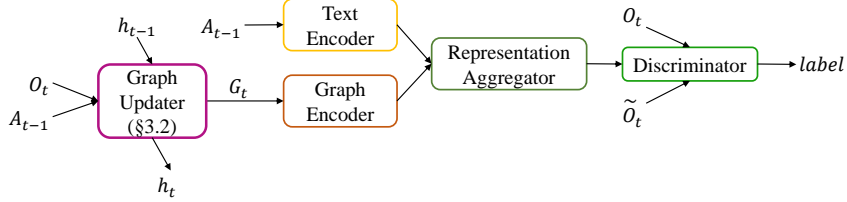


Figure 5: Contrastive observation classification model.

### B.3 Reusing Graph Encoder in Action Scorer

Both of the graph updater and action selector modules rely heavily on the graph encoder layer. It is natural to reuse the graph updater’s graph encoder during the RL training of action selector. Specifically, we use the pre-trained graph encoder (and all its dependencies such as node embeddings and relation embeddings) from either the above model to initialize the graph encoder in action selector. In such settings, we fine-tune the graph encoders during RL training. In Appendix D, we compare GATA’s performance between reusing the graph encoders with randomly initialize them.

## C GATA-GTP and Discrete Belief Graph

As mentioned in Section 3.4, since the TextWorld API provides ground-truth (discrete) KGs that describe game states at each step, we provide an agent that utilizes this information, as a strong baseline to GATA. To accommodate the discrete nature of KGs provided by TextWorld, we propose GATA-GTP, which has the same action scorer with GATA, but equipped with a discrete graph updater. We show the overview structure of GATA-GTP in Figure 6.

### C.1 Discrete Graph Updater

In the discrete graph setting, we follow [53], updating  $\mathcal{G}_t$  with a set of discrete update operations that act on  $\mathcal{G}_{t-1}$ . In particular, we model the (discrete)  $\Delta g_t$  as a set of update operations, wherein each update operation is a sequence of tokens. We define the following two elementary operations so that any graph update can be achieved in  $k \geq 0$  such operations:

- `add(node1, node2, relation)`: add a directed edge, named `relation`, between `node1` and `node2`.
- `delete(node1, node2, relation)`: delete a directed edge, named `relation`, between `node1` and `node2`. If the edge does not exist, ignore this command.

Given a new observation string  $O_t$  and  $\mathcal{G}_{t-1}$ , the agent generates  $k \geq 0$  such operations to merge the newly observed information into its belief graph.

Table 3: Update operations matching the transition in Figure 1.

---

```
<s> add player shed at <|> add shed backyard west_of <|> add wooden door shed
east_of <|> add toolbox shed in <|> add toolbox closed is <|> add workbench
shed in <|> delete player backyard at </s>
```

---

We formulate the update generation task as a sequence-to-sequence (Seq2Seq) problem and use a transformer-based model [43] to generate token sequences for the operations. We adopt the decoding strategy from [27], where given an observation sequence  $O_t$  and a belief graph  $\mathcal{G}_{t-1}$ , the agent

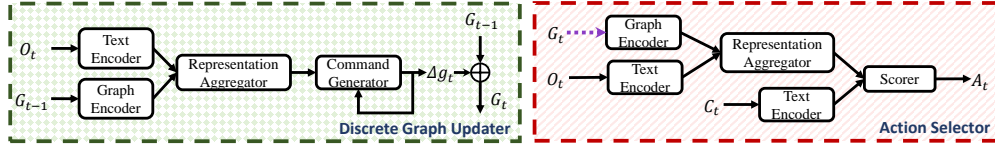


Figure 6: GATA-GTP in detail. The coloring scheme is same as in Figure 1. The **discrete graph updater** first generates  $\Delta g_t$  using  $\mathcal{G}_{t-1}$  and  $O_t$ . Afterwards the **action selector** uses  $O_t$  and the updated graph  $\mathcal{G}_t$  to select  $A_t$  from the list of action candidates  $C_t$ . Purple dotted line indicates a detached connection (i.e., no back-propagation through such connection).

generates a sequence of tokens that contains multiple graph update operations as subsequences, separated by a delimiter token  $\langle | \rangle$ .

Since Seq2Seq set generation models are known to learn better with a consistent output ordering [27], we sort the ground-truth operations (e.g., always **add** before **delete**) for training. For the transition shown in Figure 1, the generated sequence is shown in Table 3.

## C.2 Pre-training Discrete Graph Updater

As described above, we frame the discrete graph updating behavior as a language generation task. We denote this task as command generation (CG). Similar to the continuous version of graph updater in GATA, we pre-train the discrete graph updater using transitions collected from the *FTWP* dataset. It is worth mentioning that despite requiring ground-truth KGs in *FTWP* dataset, GATA-GTP does not require any ground-truth graph in the RL game to train and evaluate the action scorer.

For training discrete graph updater, we use the  $\mathcal{G}^{\text{seen}}$  type of graphs provided by the TextWorld API. Specifically, at game step  $t$ ,  $\mathcal{G}_t^{\text{seen}}$  is a discrete partial KG that contains information the agent has observed from the beginning until step  $t$ . It is only possible to train an agent to generate belief about the world it has seen and experienced.

In the collection *FTWP* transitions, every data point contains two consecutive graphs, we convert the difference between the graphs to ground-truth update operations (i.e., **add** and **delete** commands). We use standard teacher forcing technique to train the transformer-based Seq2Seq model. Specifically, conditioned on the output of representation aggregator, the command generator is required to predict the  $k^{\text{th}}$  token of the target sequence given all the ground-truth tokens up to time step  $k - 1$ . The command generator module is transformer-based decoder, similar to the observation generator described in Appendix B.1.1. Negative log-likelihood is used as loss function for optimization. An illustration of the command generation model is shown in Figure 7.



Figure 7: Command Generation Model.

During the RL training of action selector, the graph updater is detached without any back-propagation performed. It generates token-by-token started by a begin-of-sequence token, until it generates an end-of-sequence token, or hitting the maximum sequence length limit. The resulting tokens are consequently used to update the discrete belief graph.

## C.3 Pre-training a Discrete Graph Encoder for Action Scorer

In the discrete graph setting, we take advantage of the accessibility of the ground-truth graphs. Therefore we also consider various pre-training approaches to improve the performance of the graph encoder in the action selection module. Similar to the training of graph updater, we use transitions collected from the *FTWP* dataset as training data.

In particular, here we define a transition as a 6-tuple  $(\mathcal{G}_{t-1}, O_{t-1}, C_{t-1}, A_{t-1}, \mathcal{G}_t, O_t)$ . Specifically, given  $\mathcal{G}_{t-1}$  and  $O_{t-1}$ , an action  $A_{t-1}$  is selected from the candidate list  $C_{t-1}$ ; this leads to a new game state  $\mathcal{S}_t$ , thus  $\mathcal{G}_t$  and  $O_t$  are returned. Note that  $\mathcal{G}_t$  in transitions can either be  $\mathcal{G}_t^{\text{full}}$  that describes the full environment state or  $\mathcal{G}_t^{\text{seen}}$  that describes the part of state that the agent has experienced.

In this section, we start with providing details of the pre-training tasks and their corresponding models, and then show these models’ performance for each of the tasks.

### C.3.1 Action Prediction (AP)

Given a transition  $(\mathcal{G}_{t-1}, O_{t-1}, C_{t-1}, A_{t-1}, \mathcal{G}_t, O_t, r_{t-1})$ , we use  $A_{t-1}$  as positive example and use all other action candidates in  $C_{t-1}$  as negative examples. A model is required to identify  $A_{t-1}$  amongst all action candidates given two consecutive graphs  $\mathcal{G}_{t-1}$  and  $\mathcal{G}_t$ .

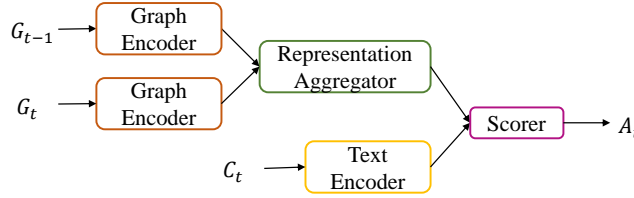


Figure 8: Action Prediction Model.

We use a model with similar structure and components as the action selector of GATA. As illustrated in Figure 8, the graph encoder first converts the two input graphs  $\mathcal{G}_{t-1}$  and  $\mathcal{G}_t$  into hidden representations, the representation aggregator combines them using attention mechanism. The list of action candidates (which includes  $A_{t-1}$  and all negative examples) are fed into the text encoder to generate action candidate representations. The scorer thus takes these representations and the aggregated graph representations as input, and it outputs a ranking over all action candidates.

In order to achieve good performance in this setting, the bi-directional attention between  $\mathcal{G}_{t-1}$  and  $\mathcal{G}_t$  in the representation aggregator needs to effectively determine the difference between the two sparse graphs. To achieve that, the graph encoder has to extract useful information since often the difference between  $\mathcal{G}_{t-1}$  and  $\mathcal{G}_t$  is minute (e.g., before and after taking an apple from the table, the only change is the location of the apple).

### C.3.2 State Prediction (SP)

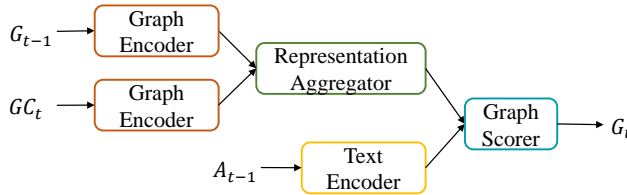


Figure 9: State Prediction Model.

Given a transition  $(\mathcal{G}_{t-1}, O_{t-1}, C_{t-1}, A_{t-1}, \mathcal{G}_t, O_t, r_{t-1})$ , we use  $\mathcal{G}_t$  as positive example and gather a set of game states by issuing all other actions in  $C_{t-1}$  except  $A_{t-1}$ . We use the set of graphs representing the resulting game states as negative samples. In this task, a model is required to identify  $\mathcal{G}_t$  amongst all graph candidates  $GC_t$  given the previous graph  $\mathcal{G}_{t-1}$  and the action taken  $A_{t-1}$ .

As shown in Figure 9, a similar model is used to train both the SP and AP tasks.

### C.3.3 Deep Graph Infomax (DGI)

This is inspired by Velickovic et al., [44]. Given a transition  $(\mathcal{G}_{t-1}, O_{t-1}, C_{t-1}, A_{t-1}, \mathcal{G}_t, O_t, r_{t-1})$ , we map the graph  $\mathcal{G}_t$  into its node embedding space. The node embedding vectors of  $\mathcal{G}_t$  is denoted as  $H$ . We randomly shuffle some of the node embedding vectors to construct a “corrupted” version of the node representations, denoted as  $\tilde{H}$ .



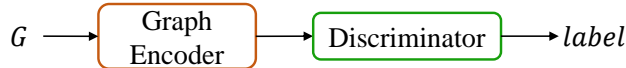


Figure 10: Deep Graph Infomax Model.

Given node representations  $H = \{\vec{h}_1, \vec{h}_2, \dots, \vec{h}_N\}$  and corrupted representations of these nodes  $\tilde{H} = \{\vec{\tilde{h}}_1, \vec{\tilde{h}}_2, \dots, \vec{\tilde{h}}_N\}$ , where  $N$  is the number of vertices in the graph, a model is required to discriminate between the original and corrupted representations of nodes. As shown in Figure 10, the model is composed of a graph encoder and a discriminator. Specifically, following [44], we utilize a noise-contrastive objective with a binary cross-entropy (BCE) loss between the samples from the joint (positive examples) and the product of marginals (negative examples). To enable the discriminator to discriminate between  $\mathcal{G}_t$  and the negative samples, the graph encoder must learn useful graph representations at both global and local level.

### C.3.4 Performance on Graph Encoder Pre-training Tasks

We provide test performance of all the models described above for graph representation learning. We fine-tune the models on validation set and report their performance on test set.

Additionally, as mentioned in Section 3.3 and Appendix A, we adapt the original R-GCN to condition the graph representation on additional information contained by the relation labels. We show an ablation study for this in Table 4, where R-GCN denotes the original R-GCN [32] and R-GCN w/ R-Emb denotes our version that considers relation labels.

Note, as mentioned in previous sections, the dataset to train, valid and test these four pre-training tasks are extracted from the *FTWP* dataset. There exist unseen nodes (ingredients in recipe) in the validation and test sets of *FTWP*, it requires strong generalizability to get decent performance on these datasets.

From Table 4, we show the relation label representation significantly boosts the generalization performance on these datasets. Compared to AP and SP, where relation label information has significant effect, both models perform near perfectly on the DGI task. This suggests the corruption function we consider in this work is somewhat simple, we leave this for future exploration.

Table 4: Test performance of models on all pre-training tasks.

Task	Graph Type	R-GCN	R-GCN w/ R-Emb
Accuracy			
AP	full	0.472	<b>0.891</b>
	seen	0.631	<b>0.873</b>
SP	full	0.419	<b>0.926</b>
	seen	0.612	<b>0.971</b>
DGI	full	0.999	<b>1.000</b>
	seen	<b>1.000</b>	<b>1.000</b>

## D Additional Results and Discussions

### D.1 Training Curves

We report the training curves of all our mentioned experiment settings. Figure 11 shows the GATA’s training curves. Figure 12 shows the training curves of the three text-based baseline (Tr-DQN, Tr-DRQN, Tr-DRQN+). Figure 13 shows the training curve of GATA-GTF (no graph updater, the action scorer takes ground-truth graphs as input) and GATA-GTP (graph updater is trained using ground-truth graphs *from the FTWP dataset*, the trained graph updater maintains a discrete belief graph throughout the RL training).

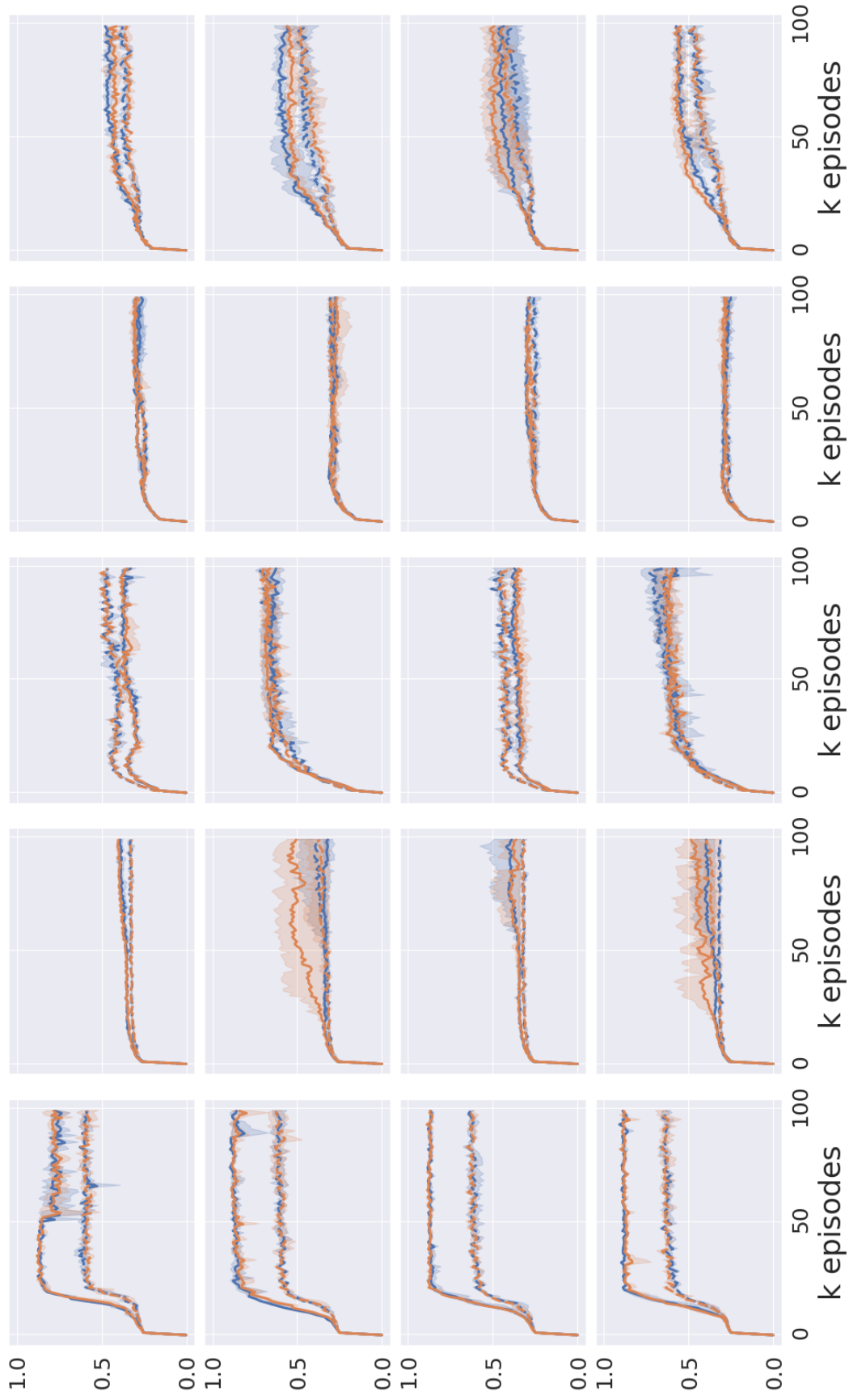


Figure 11: GATA’s training curves (averaged over 3 seeds, band represents standard deviation). Columns are difficulty levels 1/2/3/4/5. The upper two rows are GATA using belief graphs generated by the graph updater pre-trained with observation generation task; The lower two rows are GATA using belief graphs generated by the graph updater pre-trained with contrastive observation classification task. In the 4 rows, the presence of text observation are False/True/False/True. In the figure, blue lines indicate the graph encoder in action selector is randomly initialized; orange lines indicate the graph encoder in action selector is initialized by the pre-trained observation generation and contrastive observation classification tasks. Solid lines indicate 20 training games, dashed lines indicate 100 training games.

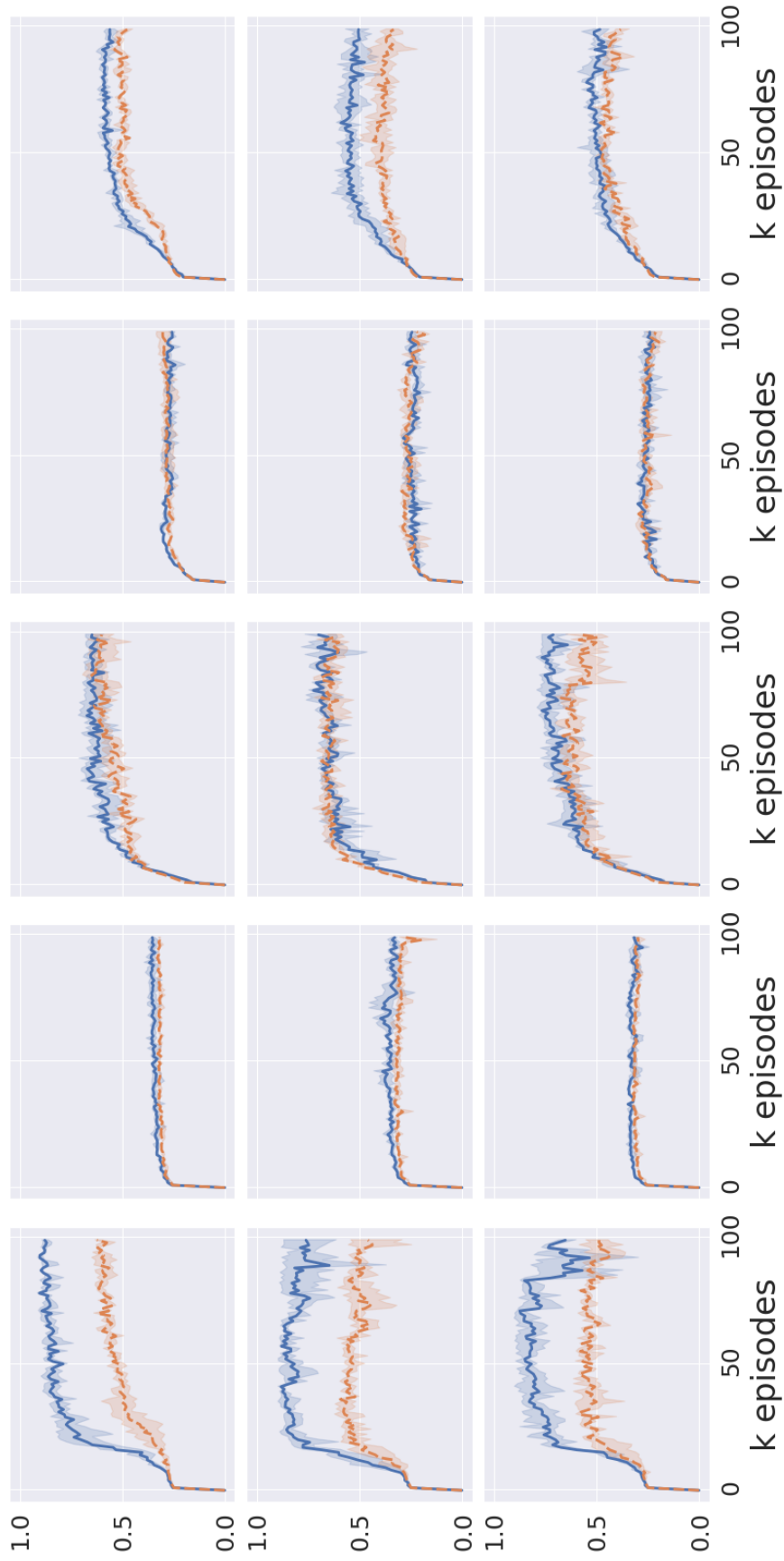


Figure 12: The text-based baseline agents' training curves (averaged over 3 seeds, band represents standard deviation). Columns are difficulty levels 1/2/3/4/5, rows are Tr-DQN, Tr-DRQN and Tr-DRQN+, respectively. All of the three agents take text observation  $O_t$  as input. In the figure, blue solid lines indicate the training set with 20 games; orange dashed lines indicate the training set with 100 games.

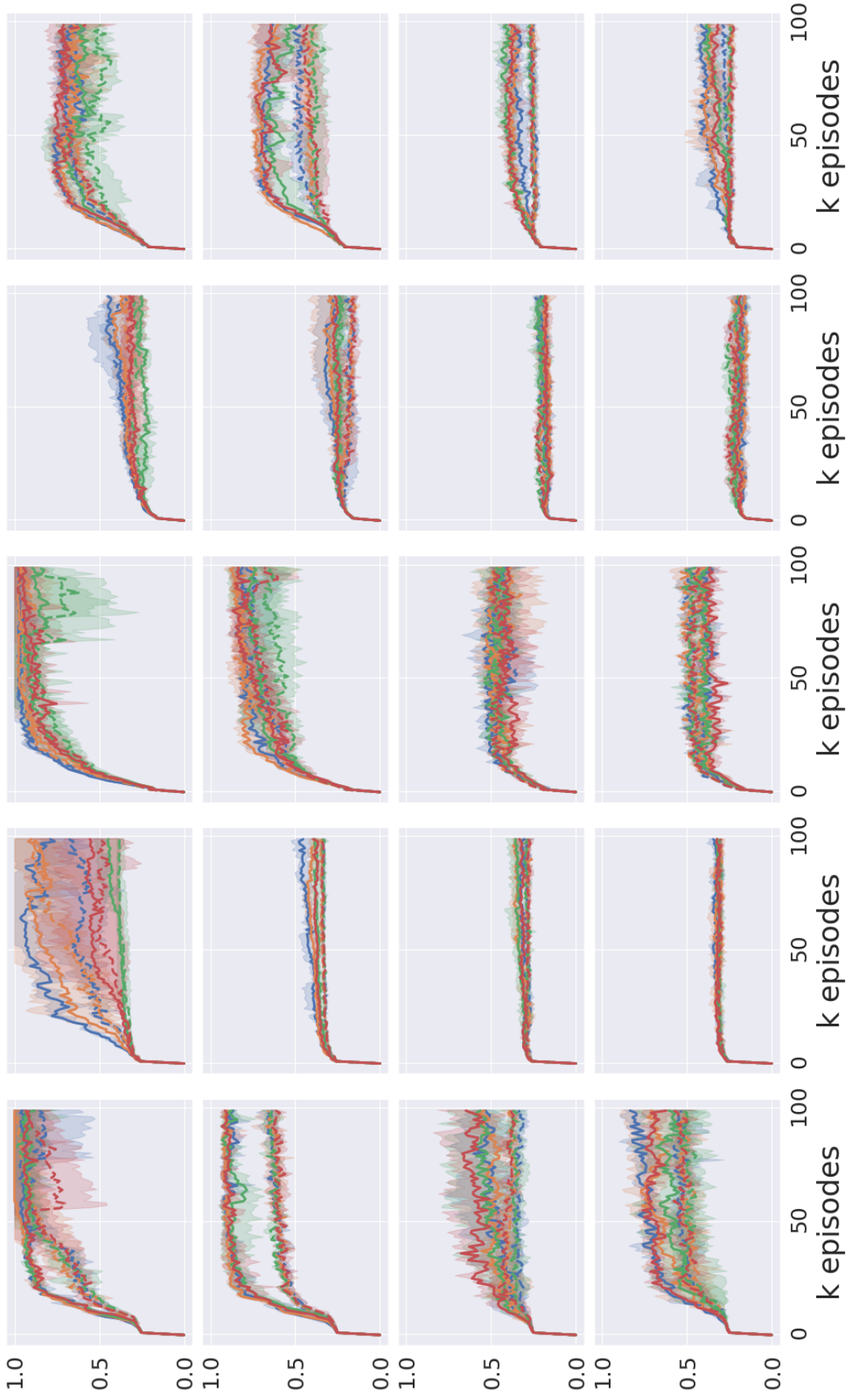


Figure 13: GATA-GTP and GATA-GTF's training curves (averaged over 3 seeds, band represents standard deviation). Columns are difficulty levels 1/2/3/4/5. The upper two rows are GATA-GTF when text observation is absent and present as input; the lower two rows are GATA-GTP when text observation is absent and present as input. In the figure, blue/orange/green indicate the agent's graph encoder is initialized with AP/SP/DGI pre-training tasks. Red lines indicate the graph encoder is randomly initialized. Solid lines indicate 20 training games, dashed lines indicate 100 training games.

## D.2 Training Scores

In Table 5 we provide all agents’ max training scores, each score is averaged over 3 random seeds. All scores are normalized. Note as described in Section 3.3, we use ground-truth KGs to train the action selector,  $\mathcal{G}^{\text{belief}}$  is only used during evaluation.

Table 5: Agents’ **Max** performance on **Training** games, averaged over 3 random seeds. In this table,  $\spadesuit$ ,  $\heartsuit$  represent  $O_t$  and  $\mathcal{G}_t^{\text{full}}$ , respectively.  $\clubsuit$  represents discrete belief graph generated by GATA-GTP (trained with ground-truth graphs of *FTWP*).  $\star$  and  $\infty$  indicate continuous belief graph generated by GATA, pre-trained with observation generation (OG) task and contrastive observation classification (COC) task, respectively. Light blue shadings represent numbers that are greater than or equal to Tr-DQN; light yellow shading represent number that are greater than or equal to all of Tr-DQN, Tr-DRQN and Tr-DRQN+.

		20 Training Games						100 Training Games						Avg.
Difficulty Level		1	2	3	4	5	% $\uparrow$	1	2	3	4	5	% $\uparrow$	% $\uparrow$
Input	Agent	Text-based Baselines												
$\spadesuit$	Tr-DQN	90.8	36.9	69.3	31.5	61.2	—	63.4	33.2	66.1	31.9	55.2	—	—
$\heartsuit$	Tr-DRQN	88.8	41.7	76.6	29.6	60.7	+2.9	60.8	33.7	71.7	30.6	44.9	-3.4	-0.2
$\clubsuit$	Tr-DRQN+	89.1	35.6	78.0	30.9	58.1	+0.0	61.1	32.8	70.0	30.0	50.3	-2.8	-1.4
Pre-training		GATA												
$\star$	N/A	87.9	40.4	40.1	30.8	50.1	-11.2	65.1	34.6	51.2	32.0	41.8	-7.9	-9.6
$\star$	OG	88.8	40.8	40.1	32.1	48.2	-10.6	63.8	33.9	51.9	32.6	39.3	-9.1	-9.8
$\star\spadesuit$	N/A	90.2	35.4	69.0	32.0	62.8	-0.2	63.9	41.2	72.2	32.2	50.8	+5.4	+2.6
$\star\spadesuit$	OG	90.0	57.1	70.6	31.7	57.9	+10.2	64.2	38.9	72.5	32.4	50.1	+4.1	+7.1
$\infty$	N/A	89.0	43.1	41.2	31.8	48.7	-9.0	65.8	33.4	51.5	29.1	44.0	-9.4	-9.2
$\infty$	COC	89.6	41.0	39.2	31.9	54.4	-8.7	65.8	33.4	48.6	31.2	47.2	-7.8	-8.2
$\infty\spadesuit$	N/A	90.9	41.4	66.1	31.3	58.8	+0.6	67.1	33.1	73.6	29.9	51.2	+0.7	+0.6
$\infty\spadesuit$	COC	90.2	50.8	66.4	31.9	59.3	+6.2	67.4	41.5	66.6	31.4	50.8	+4.5	+5.4
		GATA-GTP												
$\clubsuit$	N/A	73.3	34.5	50.5	21.7	43.5	-22.6	49.3	31.1	54.3	25.1	28.8	-23.1	-22.8
$\clubsuit$	AP	68.4	34.8	61.3	23.8	43.1	-19.2	40.9	31.3	55.4	24.8	28.8	-25.7	-22.4
$\clubsuit$	SP	62.7	38.1	57.5	23.5	44.1	-19.6	50.2	30.8	55.0	23.7	28.0	-24.0	-21.8
$\clubsuit$	DGI	64.9	37.0	55.6	25.7	47.4	-17.8	43.4	31.8	58.3	25.3	30.2	-22.7	-20.3
$\clubsuit\spadesuit$	N/A	77.5	33.9	45.6	26.3	40.2	-21.6	59.5	32.3	55.4	29.1	27.6	-16.8	-19.2
$\clubsuit\spadesuit$	AP	87.5	35.8	50.4	22.3	45.4	-17.8	61.3	32.2	56.3	25.3	33.0	-16.4	-17.1
$\clubsuit\spadesuit$	SP	80.0	35.5	50.2	23.5	44.0	-19.4	57.3	32.1	58.3	27.1	29.2	-17.4	-18.4
$\clubsuit\spadesuit$	DGI	70.3	33.9	51.4	26.3	42.1	-20.9	57.7	32.7	55.6	28.8	29.8	-16.4	-18.6
		GATA-GTF												
$\heartsuit$	N/A	98.6	58.4	95.6	36.1	80.9	+30.3	96.0	53.4	97.9	36.0	76.4	+42.3	+36.3
$\heartsuit$	AP	98.7	97.5	98.3	48.1	79.3	+59.4	97.1	74.7	98.3	44.5	75.9	+60.8	+60.1
$\heartsuit$	SP	100.0	96.9	98.3	44.9	76.6	+56.5	98.6	90.5	99.0	38.9	73.4	+66.6	+61.5
$\heartsuit$	DGI	96.9	45.4	95.3	28.7	72.6	+15.4	98.2	39.1	90.1	33.0	62.4	+25.1	+20.2
$\heartsuit\spadesuit$	N/A	91.7	55.9	80.9	33.6	63.2	+15.8	73.5	48.1	67.7	31.8	56.7	+13.1	+14.5
$\heartsuit\spadesuit$	AP	87.9	62.4	78.8	32.4	62.8	+17.0	76.8	54.0	73.7	34.1	55.6	+20.6	+18.8
$\heartsuit\spadesuit$	SP	90.7	55.8	83.8	30.7	64.2	+14.9	60.4	40.1	67.4	31.1	51.5	+1.8	+8.3
$\heartsuit\spadesuit$	DGI	88.1	38.1	73.0	32.5	62.5	+2.2	66.4	35.5	59.1	30.4	49.6	-2.8	-0.3

### D.3 Test Results

In Table 6 we provide all our agent variants and the text-based baselines’ test scores. We report agents’ test score corresponding to their best validation scores.

Table 6: Agents’ performance on **test** games, model selected using best validation performance. **Boldface** and underline represent the highest and second highest values in a setting (excluding GATA-GTF which has access to the ground-truth graphs of the RL games). In this table, ♣, ♦ represent  $O_t$  and  $\mathcal{G}_t^{\text{full}}$ , respectively. ♣ represents discrete belief graph generated by GATA-GTP (pre-trained with ground-truth graphs of *FTWP*). ★ and ∞ indicate continuous belief graph generated by GATA, pre-trained with observation generation (OG) task and contrastive observation classification (COC) task, respectively. Light blue shadings represent numbers that are greater than or equal to Tr-DQN; light yellow shading represent number that are greater than or equal to all of Tr-DQN, Tr-DRQN and Tr-DRQN+.

		20 Training Games							100 Training Games							Avg.
Difficulty Level		1	2	3	4	5	% ↑	1	2	3	4	5	% ↑	% ↑		
Input	Agent	Text-based Baselines														
♣	Tr-DQN	66.2	26.0	16.7	18.2	<b>27.9</b>	—	62.5	32.0	38.3	17.7	34.6	—	—		
♣	Tr-DRQN	62.5	32.0	28.3	12.7	26.5	+10.3	58.8	31.0	36.7	21.4	27.4	-2.6	+3.9		
♣	Tr-DRQN+	65.0	30.0	35.0	11.8	18.3	+10.7	58.8	33.0	33.3	19.5	30.6	-3.4	+3.6		
Pre-training		GATA														
★	N/A	70.0	20.0	20.0	18.6	26.3	-0.2	62.5	32.0	46.7	<b>27.7</b>	35.4	+16.1	+8.0		
★	OG	66.2	28.0	21.7	15.9	24.3	+2.4	<u>66.2</u>	34.0	40.0	21.4	34.0	+7.2	+4.8		
★♣	N/A	66.2	34.0	30.0	12.7	24.3	+13.5	<u>66.2</u>	<b>38.0</b>	36.7	<u>27.3</u>	36.1	+15.8	+14.6		
★♣	OG	66.2	<b>48.0</b>	26.7	15.5	26.3	+24.8	<u>66.2</u>	<u>36.0</u>	<b>58.3</b>	14.1	<b>45.0</b>	+16.1	+20.4		
∞	N/A	73.8	42.0	26.7	<b>20.9</b>	24.5	+27.1	62.5	30.0	51.7	23.6	36.0	+13.2	+20.2		
∞	COC	66.2	29.0	30.0	18.2	<u>27.7</u>	+18.1	<u>66.2</u>	34.0	41.7	19.1	<u>40.3</u>	+9.1	+13.6		
∞♣	N/A	68.8	33.0	<u>41.7</u>	17.7	27.0	+34.9	62.5	33.0	46.7	25.9	33.4	+13.6	+24.2		
∞♣	COC	66.2	<u>44.0</u>	16.7	<u>20.0</u>	21.7	+11.4	<b>70.0</b>	34.0	45.0	12.3	36.2	+2.0	+6.7		
		GATA-GTP														
♣	N/A	56.2	23.0	<u>41.7</u>	11.4	22.1	+13.0	45.0	32.0	30.0	10.5	17.4	-28.0	-7.5		
♣	AP	50.0	20.0	25.0	9.5	24.3	-11.7	45.0	31.0	50.0	15.9	24.4	-8.0	-9.9		
♣	SP	45.0	25.0	38.3	11.8	22.6	+7.9	42.5	32.0	50.0	11.4	22.5	-14.4	-3.3		
♣	DGI	56.2	26.0	40.0	17.3	17.7	+16.6	37.5	31.0	45.0	13.6	18.7	-18.9	-1.2		
♣♣	N/A	<u>73.8</u>	31.0	28.3	8.2	22.5	+5.2	62.5	29.0	38.3	13.2	19.8	-15.5	-5.2		
♣♣	AP	62.5	32.0	<b>46.7</b>	12.3	21.1	+28.1	58.8	30.0	40.0	10.9	29.2	-12.4	+7.9		
♣♣	SP	65.0	32.0	<u>41.7</u>	12.3	23.5	+24.6	62.5	32.0	51.7	21.8	23.5	+5.2	+14.9		
♣♣	DGI	<b>75.0</b>	27.0	33.3	17.3	24.3	+19.7	62.5	31.0	46.7	19.5	24.7	+0.1	+9.9		
		GATA-GTF														
♦	N/A	83.8	53.0	33.3	23.6	24.8	+49.7	100.0	90.0	68.3	37.3	52.7	+96.5	+73.1		
♦	AP	85.0	39.0	26.7	26.4	27.5	+36.4	92.5	88.0	63.3	53.6	51.6	+108.0	+72.2		
♦	SP	48.7	61.0	46.7	23.6	28.9	+64.2	95.0	95.0	70.0	37.3	52.8	+99.0	+81.6		
♦	DGI	85.0	27.0	31.7	14.1	22.1	+15.7	100.0	40.0	70.0	31.8	50.6	+58.7	+37.2		
♦♣	N/A	92.5	39.0	30.0	15.9	23.6	+28.3	96.3	56.0	55.0	14.5	46.6	+37.9	+33.1		
♦♣	AP	73.8	36.0	46.7	25.9	23.9	+51.5	85.0	42.0	68.3	36.4	47.5	+57.7	+54.6		
♦♣	SP	62.5	24.0	36.7	14.5	28.6	+17.7	60.0	43.0	46.7	25.0	47.9	+26.4	+21.1		
♦♣	DGI	81.2	30.0	25.0	16.8	30.7	+18.0	73.8	39.0	48.3	15.0	40.6	+13.6	+15.8		



## D.4 Other Remarks

**Pre-training graph encoder helps.** In Table 5 and Table 6, we also show GATA, GATA-GTP and GATA-GTF’s training and test scores when their action scorer’s graph encoder are initialized with pre-trained parameters as introduced in Section 3.2 (for GATA) and Appendix C.3 (for GATA-GTP and GATA-GTF). We observe in most settings, pre-trained graph encoders produce better training and test results compared to their randomly initialized counterparts. This is particularly obvious in GATA-GTP and GATA-GTF, where graphs are discrete. For instance, from Table 6 we can see that only with text observation as additional input ( $\clubsuit\clubsuit$ ), and when graph encoder are initialized with AP/SP/DGI, the GATA-GTP agent can outperform the text-based baselines on test game sets.

**Fine-tuning graph encoder helps.** For all experiment settings where the graph encoder in action scorer is initialized with pre-trained parameters (OG/COC for GATA, AP/SP/DGI for GATA-GTP), we also compare between freezing vs. fine-tuning the graph encoder in RL training. By freezing the graph encoders, we can effectively reduce the number of parameters to be optimized with RL signal. However, we see consistent trends that fine-tuning the graph encoders can always provide better training and testing performance in both GATA and GATA-GTP.

**Text input helps more when graphs are imperfect.** We observe clear trends that for GATA-GTF, using text together with graph as input (to the action selector) does not provide obvious performance increase. Instead, GATA-GTF often shows better performance when text observation input is disabled. This observation is coherent with the intuition of using text observations as additional input. When the input graph to the action selector is imperfect (e.g., belief graph maintained by GATA or GATA-GTP itself), the text observation provides more accurate information to help the agent to recover from errors. On the other hand, GATA-GTF uses the ground-truth full graph (which is even accurate than text) as input to the action selector, the text observation might confuse the agent by providing redundant information with more uncertainty.

**Learning across difficulty levels.** We have a special set of RL games — level 5 — which is a mixture of the other four difficulty levels. We use this set to evaluate an agent’s generalizability on both dimensions of game configurations and difficulty levels. From Table 5, we observe that almost all agents (including baseline agents) benefit from a larger training set, i.e., achieve better test results when train on 100 level 5 games than 20 of them. Results show GATA has a more significant performance boost from larger training set. We notice that all GATA-GTP variants perform worse than text-based baselines on level 5 games, whereas GATA outperforms text-based baselines when training on 100 games. This may suggest the continuous belief graphs can better help GATA to adapt to games across difficulty levels, whereas its discrete counterpart may struggle more. For example, both games in level 1 and 2 have only single location, while level 3 and 4 games have multiple locations. GATA-GTP might thus get confused since sometimes the direction relations (e.g., *west\_of*) are unused. In contrast, GATA, equipped with continuous graphs, may learn such scenario easier.

## D.5 Probing Task and Belief Graph Visualization

In this section, we investigate whether generated belief graphs contain any useful information about the game dynamics. We first design a probing task to check if  $\mathcal{G}$  encodes the existing relations between two nodes. Next, we visualize a few slices of the adjacency tensor associated to  $\mathcal{G}$ .

### D.5.1 Probing Task

We frame the probing task as a multi-label classification of the relations between a pair of nodes. Concretely, given two nodes  $i, j$ , and the vector  $\mathcal{G}_{i,j} \in [-1, 1]^{\mathcal{R}}$  (in which  $\mathcal{R}$  denotes the number of relations) extracted from the belief graph  $\mathcal{G}$  corresponding to the nodes  $i$  and  $j$ , the task is to learn a function  $f$  such that it minimizes the following binary cross-entropy loss:

$$\mathcal{L}_{\text{BCE}}(f(\mathcal{G}_{i,j}, h_i, h_j), Y_{i,j}), \quad (15)$$

where  $h_i, h_j$  are the embeddings for nodes  $i$  and  $j$ ,  $Y_{i,j} \in \{0, 1\}^{\mathcal{R}}$  is a binary vector representing the presence of each relation between the nodes (there are  $R$  different relations). Following Alain and Bengio [2], we use a linear function as  $f$ , since we assume the useful information should be easily accessible from  $\mathcal{G}$ .

Table 7: Probing task results showing that belief graphs obtained from OG and COC do contain information about the game dynamics, i.e. node relationships.

Model	Exact Match						F <sub>1</sub> score					
	Train			Test			Train			Test		
	+	-	Avg	+	-	Avg	+	-	Avg	+	-	Avg
Random	0.00	0.99	0.49	0.00	0.99	0.49	0.00	0.99	0.49	0.00	0.99	0.49
Ground-truth	0.98	0.96	0.97	0.97	0.96	0.97	0.98	0.96	0.97	0.98	0.96	0.97
Tr-DRQN	0.61	0.84	0.73	0.61	0.83	0.72	0.61	0.84	0.73	0.61	0.83	0.72
GATA (OG)	0.69	0.86	<b>0.78</b>	0.70	0.86	<b>0.78</b>	0.71	0.85	<b>0.78</b>	0.72	0.86	<b>0.79</b>
GATA (COC)	0.65	0.86	0.75	0.65	0.84	0.75	0.67	0.85	0.76	0.67	0.84	0.75

We collect a dataset for this probing task by following the walkthroughs of 120 games. At every game step, we collect a tuple  $(\mathcal{G}, \mathcal{G}^{\text{seen}})$  (see Appendix C.2 for the definition of  $\mathcal{G}^{\text{seen}}$ ). We used tuples from 100 games as training data and the remaining for evaluation.

From each tuple in the dataset, we extract several node pairs  $(i, j)$  and their corresponding  $Y_{i,j}$  from  $\mathcal{G}^{\text{seen}}$  (positive examples, denoted as “+”). To make sure a model can only achieve good performance on this probing task by using the belief graph  $\mathcal{G}$ , without overfitting by memorising node-relation pairs (e.g., the unique relation between player and kitchen is **at**), we augment the dataset by adding plausible node pairs (i.e.,  $Y_{i,j} = \vec{0}^{\mathcal{R}}$ ) but that have no relation according to the current  $\mathcal{G}$  (negative examples, denoted as “-”). For instance, if at a certain game step the player is in the bedroom, the relation between the player and kitchen should be empty ( $\vec{0}^{\mathcal{R}}$ ). We expect  $\mathcal{G}$  to have captured that information.

We use two metrics to evaluate the performance on this probing task:

- **Exact match** represents the percentage of predictions that have all their labels classified correctly, i.e., when  $f(\mathcal{G}_{i,j}, h_i, h_j) = Y_{i,j}^n$ .
- **F<sub>1</sub> score** which is the harmonic mean between precision and recall. We report the macro-averaging of F<sub>1</sub> over all the predictions.

To better understand the probe’s behaviors on each settings, we also report their training and test performance on the positive samples (+) and negative samples (-) separately.

From Table 7, we observe that belief graphs  $\mathcal{G}$  generated by models pre-trained with either OG or COC do contain useful information about the relations between a pair of nodes. We first compare against a random baseline where each  $\mathcal{G}$  is randomly sampled from  $\mathcal{N}(0, 1)$  and kept fixed throughout the probing task. We observe the linear probe fails to perform well on the training set (and as a result also fails to generalize on test set). Interestingly, with random belief graphs provided, the probe somehow overfits on negative samples and always outputs zeros all the time. In both training and testing phases, it produces zero performance on positive examples. This baseline suggests the validity of our probing task design — there is no way to correctly predict the relations without having the information encoded in the belief graph  $\mathcal{G}$ .

Next, we report the performance of using ground-truth graphs ( $\mathcal{G}^{\text{seen}}$ ) as input to  $f$ . We observe the linear model can perform decently on training data, and can generalize from training to testing data — on both sets, the linear probe achieves near-perfect performance. This also verifies the probing task by showing that given the ground-truth knowledge, the linear probe is able to solve the task easily.

Given the two extreme cases as upper bound and lower bound, we investigate the belief graphs  $\mathcal{G}$  generated by GATA, pre-trained with either of the two self-supervised methods, OG and COC (proposed in Section 3.2). From Table 7, we can see  $\mathcal{G}$  generated by both OG and COC methods help similarly in the relation prediction task, both provide more than 75% of testing exact match scores.

In Section 4, we show that GATA outperforms a set of baseline systems, including Tr-DRQN (as described in Section 4.1), an agent with recurrent components. To further investigate if the belief graphs generated by GATA can better facilitate the linear probe in this relation prediction task, we provide an additional setting. We modify the Tr-DRQN agent by replacing its action scorer by a text generator (the same decoder used in OG training), and train this model with the same data and objective as OG. After pre-training, we obtain a set of probing data by collecting the recurrent hidden states produced by this agent given the same probing game walkthroughs. Since these recurrent

hidden states are computed from the same amount of information as GATA’s belief graphs, they could theoretically contain the same information as  $\mathcal{G}$ . However, from Table 7, we see that the scores of Tr-DRQN are consistently lower than GATA’s score. This is coherent with our findings in the RL experiments (Section 4), except the gap between GATA and Tr-DRQN is less significant in the relation prediction task setting.

While being able to perform the classification correctly in a large portion of examples, we observe a clear performance gap comparing GATA’s belief graphs with ground-truth graphs. The cause of the performance gap can be twofold. First, compared to ground-truth graphs that accurately represent game states without information loss,  $\mathcal{G}$  (iteratively generated by a neural network across game steps) can inevitably suffer from information loss. Second, the information encoded in  $\mathcal{G}$  might not be easily extracted by a linear probe (compared to ground-truth). Both aspects suggest potential future directions to improve the belief graph generation module.

We optimize all probing models for 10 epochs with Adam optimizer, using the default hyperparameters and a learning rate of 0.0001. Note in all the probing models, only parameters of the linear layer  $f$  are trainable, everything else (including node embeddings) are kept fixed.

### D.5.2 Belief Graph Visualization

In Figure 14, we show a slice of the ground-truth adjacency tensor representing the `is` relation. To give context, that tensor has been extracted at the end of a game with a recipe requesting a fried diced red apple, a roasted sliced red hot pepper, and a fried sliced yellow potato. Correspondingly, for the same game and same time step, Figure 15 shows the same adjacency tensor’s slice for the belief graphs  $\mathcal{G}$  generated by GATA pre-trained on observation generation (OG) and contrastive observation classification (COC) tasks.

For visualization, we found that subtracting the mean adjacency tensor, computed across all games and steps, helps by removing information about the marginal distribution of the observations (e.g., underlying grammar or other common features needed for the self-supervised tasks). Those “cleaner” graphs are shown in Figure 16. One must keep in mind that there is no training signal to force the belief graphs to align with any ground-truth graphs since the belief graph generators are trained with pure self-supervised methods.

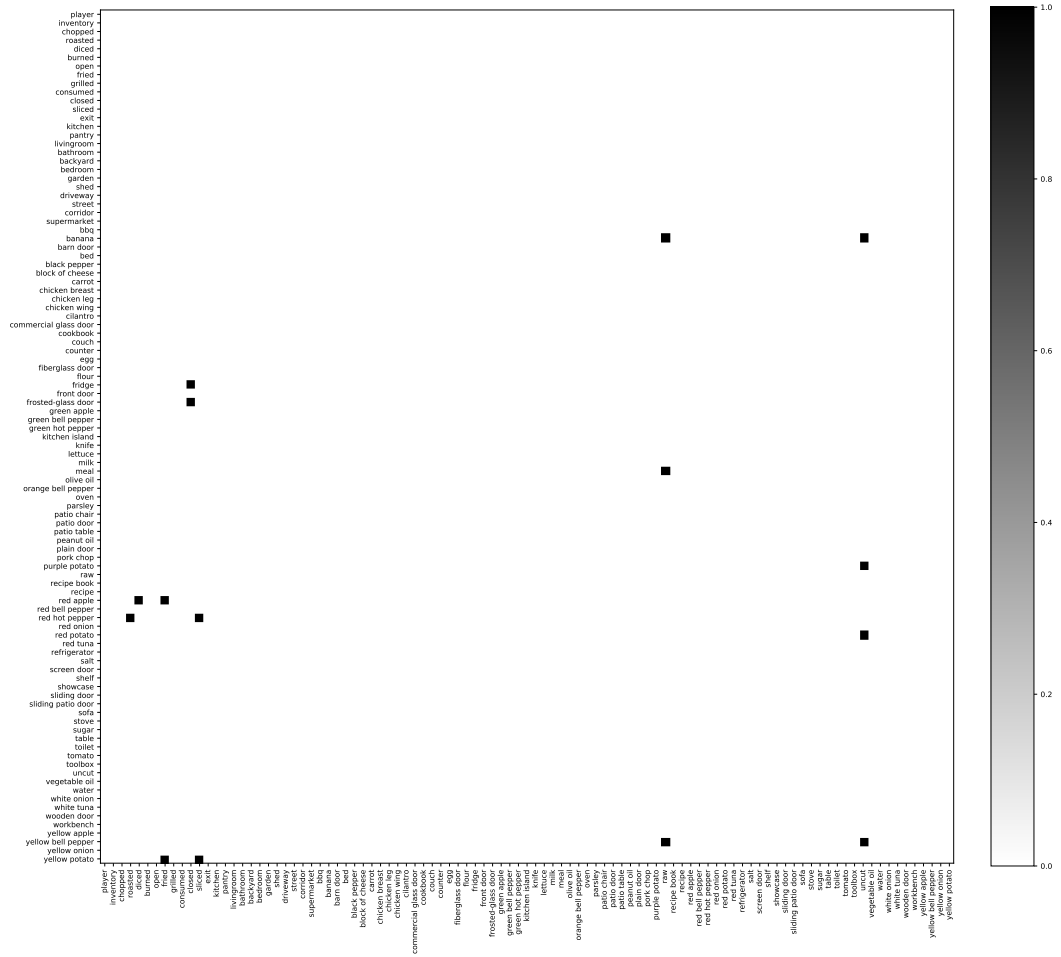


Figure 14: Slice of a ground-truth adjacency tensor representing the *is* relation.

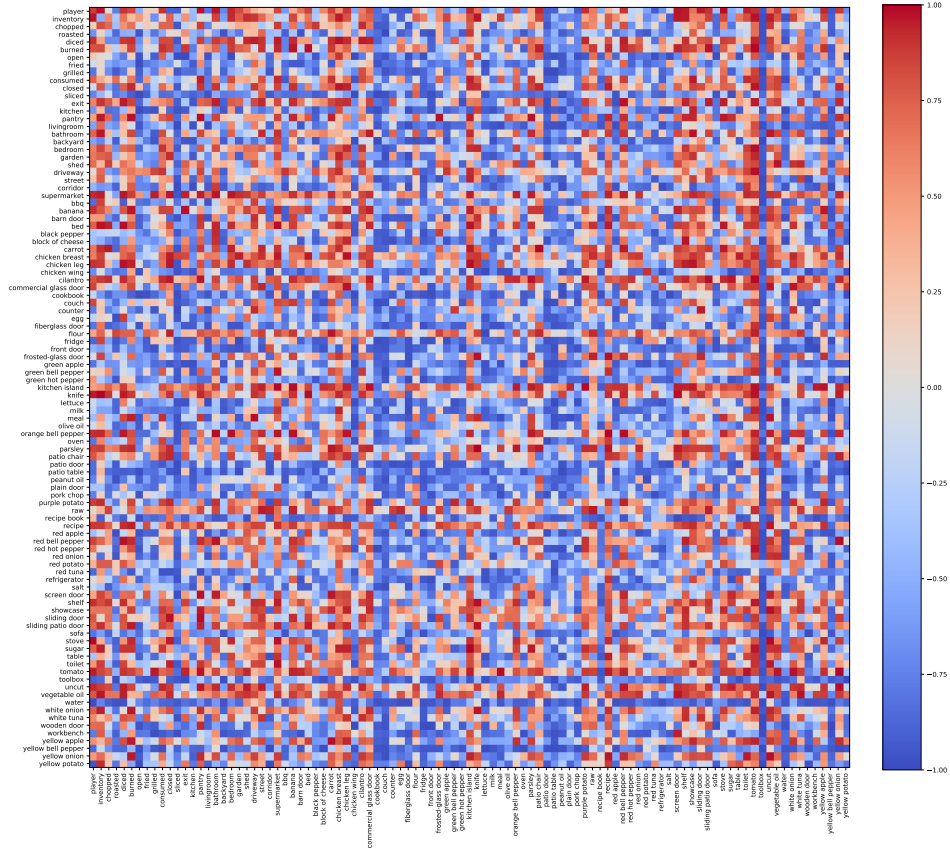
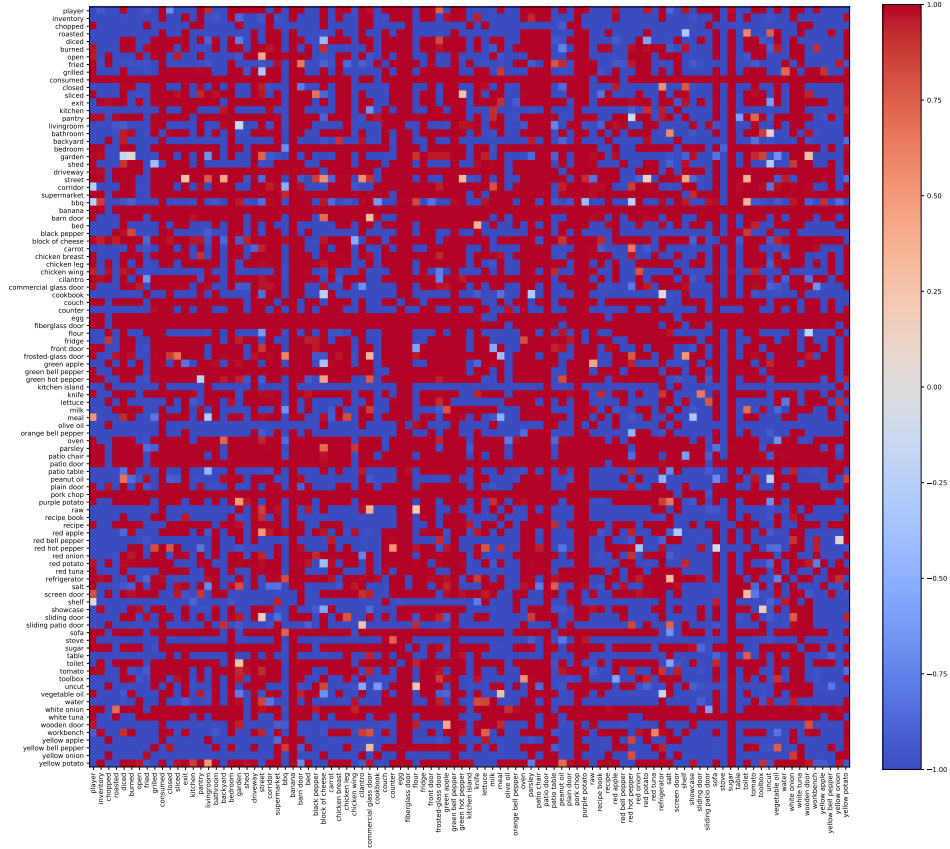


Figure 15: Adjacency tensor’s slices for  $\mathcal{G}$  generated by GATA, pre-trained with OG task (**top**) and COC task (**bottom**).

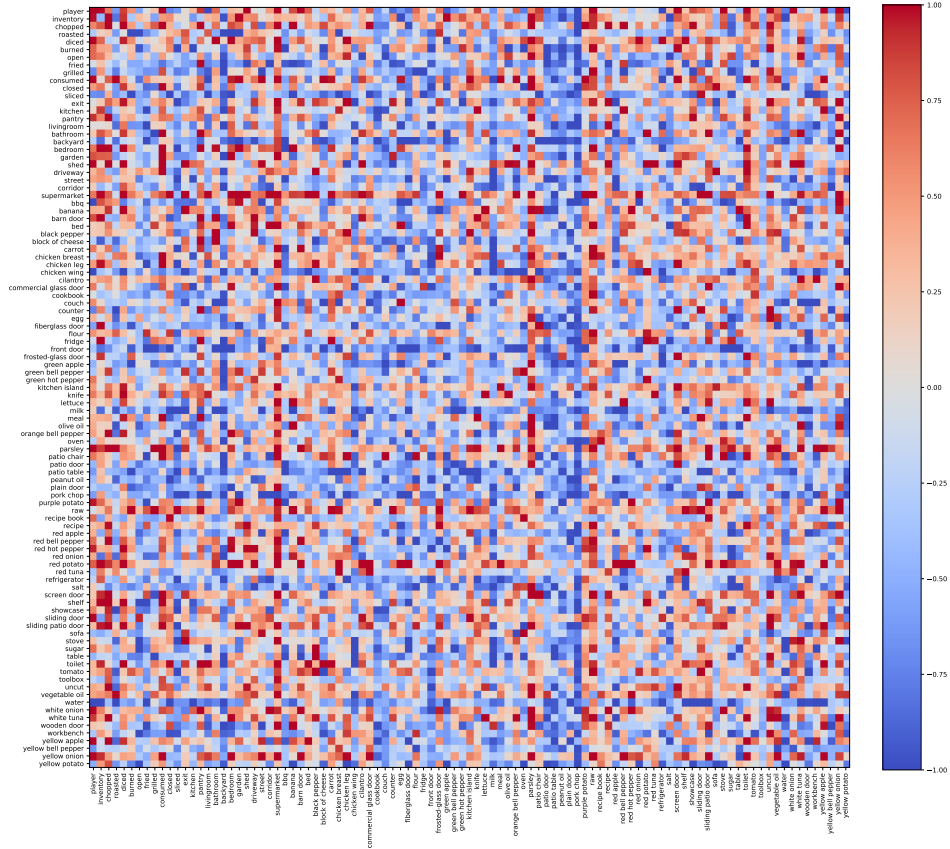
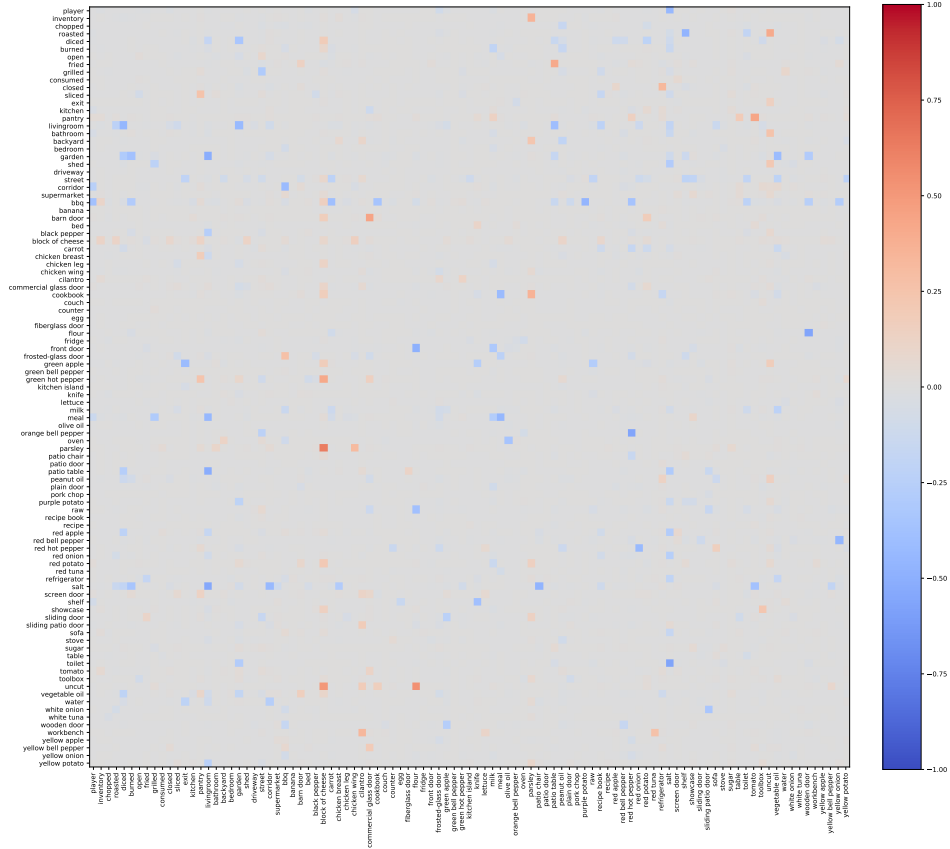


Figure 16: Adjacency tensor’s slices after subtracting the mean for  $\mathcal{G}$  generated by GATA, pre-trained with OG task (top) and COC task (bottom).



Table 8: Selected example of test set of the observation generation task. On this specific data point, The model gets an  $F_1$  score of 0.64. We use same colors to shade the information overlap between ground-truth observation with the model prediction.

Ground-Truth
<p>                     -= kitchen = - of every kitchen you could have sauntered into , you had to saunter into a normal one . you can make out a fridge .                      the fridge contains a raw chicken wing , a raw chicken leg and a block of cheese . you can make out an oven . you hear a noise                      behind you and spin around , but you ca n't see anything other than a table . wow , is n't textworld just the best ? you see a cookbook                      on the table . hmmm ... what else , what else ? you make out a counter . now why would someone leave that there ? the counter is vast .                      on the counter you make out a raw purple potato and a knife . you can make out a stove . the stove is conventional . unfortunately ,                      there is n't a thing on it . hopefully this does n't make you too upset . there is an open frosted - glass door leading east . there is an                      exit to the north . do n't worry , there is no door . you need an exit without a door ? you should try going west . there is a white onion                      on the floor .                 </p>
Prediction
<p>                     -= kitchen = - you 're now in a kitchen . you begin looking for stuff . you can make out a fridge . the fridge contains a raw chicken                      leg . you can make out a closed oven . you can make out a table . the table is massive . on the table you see a knife . you see a                      counter . the counter is vast . on the counter you can make out a cookbook . you can make out a stove . the stove is conventional .                      but the thing has n't got anything on it . you can make out a stove . the stove is conventional . but the thing has n't got anything on it .                      there is an open frosted - glass door leading east . there is an exit to the east .                 </p>

## D.6 GATA’s Performance on Graph Updater Pre-training Tasks

In this subsection, we report the test performance of the two graph updater pre-training tasks for GATA.

In the observation generation (OG) task, our model achieves a test loss of 22.28 (when using ground-truth history tokens as input to the decoder), and a test  $F_1$  score of 0.68 (when using the previously generated token as input to the decoder).

In the contrastive observation classification (COC) task, our model achieves a test loss of 0.06, and a test accuracy of 0.97.

In Table 8, we show a selected test example from the observation generation task. In the example, the prediction has fair amount of overlap (semantically, not necessarily word by word) with the ground-truth. This suggests the belief graph  $\mathcal{G}_t^{\text{belief}}$  generated by GATA’s updater model can to some extent capture and encode the state information of the environment — since the model is able to reconstruct  $O_t$  using  $\mathcal{G}_t^{\text{belief}}$ .

## D.7 Future Directions

As mentioned in Appendix D.5, the belief graphs generated by GATA lack of interpretability because the training is not supervised by any ground-truth graph. Technically, they are recurrent hidden states that encode the game state, we only (weakly) ground these real-valued graphs by providing node and relation vocabularies (word embeddings) for the message passing in R-GCN.

Therefore, there can be two potential directions deriving from the current approach. First, it would be interesting to investigate regularization methods and auxiliary tasks that can make the belief graph sparser (without relying on ground-truth graphs to train). A sparser belief graph may increase GATA’s interpretability, however, it does not guarantee to produce better performance on playing text-based games (which is what we care more about).

Second, it would also be interesting to see how GATA can be adapted to environments where the node and relation names are unknown. This will presumably make the learned belief graphs even far away from interpretable, but at the same time it will further relax GATA from the need of requiring any prior knowledge about the environments. We believe this is an essential property for an agent that is generalizable to out-of-distribution environments. For instance, without the need of a pre-defined node and relation vocabularies, we can expand GATA to the setting where training on the cooking games, and testing on games from another genre, or even text-based games designed for humans [14].

---

**Algorithm 1** Training Strategy for GATA Action Selector

---

```
1: Input: games  $\mathcal{X}$ , replay buffer  $B$ , update frequency  $F$ , patience  $P$ , tolerance  $\tau$ , evaluation frequency  $E$ .
2: Initialize counters  $k \leftarrow 1, p \leftarrow 0$ , best validation score  $V \leftarrow 0$ , transition cache  $C$ , policy  $\pi$ , checkpoint  $\Pi$ .
3: for  $e \leftarrow 1$  to NB_EPISODES do
4:   Sample a game  $x \in \mathcal{X}$ , reset  $C$ .
5:   for  $i \leftarrow 1$  to NB_STEPS do
6:     play game, push transition into  $C$ ,  $k \leftarrow k + 1$ 
7:     if  $k \% F = 0$  then sample batch from  $B$ , Update( $\pi$ )
8:     if done then break
9:   end for
10:  if average score in  $C > \tau \cdot$  average score in  $B$  then
11:    for all item in  $C$  do push item into  $B$ 
12:  end if
13:  if  $e \% E \neq 0$  then continue
14:   $v \leftarrow$  Evaluate( $\pi$ )
15:  if  $v \geq V$  then  $\Pi \leftarrow \pi, p \leftarrow 0$ , continue
16:  if  $p > P$  then  $\pi \leftarrow \Pi, p \leftarrow 0$ 
17:  else  $p \leftarrow p + 1$ 
18: end for
```

---

## E Implementation Details

In Appendix A, we have introduced hyperparameters regarding model structures. In this section, we provide hyperparameters we used in training and optimizing.

In all experiments, we use *Rectified Adam* [25] as the step rule for optimization. The learning rate is set to 0.001. We clip gradient norm of 5.

### E.1 Graph Updater

To pre-train the recurrent graph updater in GATA, we utilize the backpropagation through time (BPTT) algorithm. Specifically, we unfold the recurrent graph updater and update every 5 game steps. We freeze the parameters in graph updater after its own training process. Although it can theoretically be trained on-the-fly together with the action selector (with reward signal), we find the standalone training strategy more effective and efficient.

### E.2 Action Selector

The overall training procedure of GATA’s action selector is shown in Algorithm 1.

We report two strategies that we empirically find effective in DQN training. First, we discard the underachieving trajectories without pushing them into the replay buffer (lines 10–12). Specifically, we only push a new trajectory that has an average reward greater than  $\tau \in \mathbb{R}_0^+$  times the average reward for all transitions in the replay buffer. We use  $\tau = 0.1$ , since it keeps around some weaker but acceptable trajectories and does not limit exploration too severely. Second, we keep track of the best performing policy  $\Pi$  on the validation games. During training, when GATA stops improving on validation games, we load  $\Pi$  back to the training policy  $\pi$  and resume training. After training, we report the performance of  $\Pi$  on test games. Note these two strategies are not designed specifically for GATA; rather, we find them effective in DQN training in general.

We use a prioritized replay buffer with memory size of 500,000, and a priority fraction of 0.6. We use  $\epsilon$ -greedy, where the value of  $\epsilon$  anneals from 1.0 to 0.1 within 20,000 episodes. We start updating parameters after 100 episodes of playing. We update our network after every 50 game steps (update frequency  $F$  in Algorithm 1)<sup>7</sup>. During update, we use a mini-batch of size 64. We use a discount  $\gamma = 0.9$ . We update target network after every 500 episodes. For multi-step learning, we sample the multi-step return  $n \sim \text{Uniform}[1, 3]$ . We refer readers to Hessel et al. [18] for more information about different components of DQN training.

---

<sup>7</sup>50 is the total steps performed within a batch. For instance, when batch size is 1, we update per 50 steps; whereas when batch size is 10, we update per 5 steps. Note the batch size here refers to the parallelization of the environment, rather than the batch size for backpropagation.

In our implementation of the Tr-DRQN and Tr-DRQN+ baselines, following Yuan et al. [50], we sample a sequence of transitions of length 8, use the first 4 transitions to estimate reasonable recurrent states and use the last for to update. For counting bonus, we use a  $\gamma_c = 0.5$ , the bonus is scaled by an coefficient  $\lambda_c = 0.1$ .

For all experiment settings, we train agents for 100,000 episodes (NB\_EPISODES in Algorithm 1). For each game, we set maximum step of 50 (NB\_STEPS in Algorithm 1). When an agent has used up all its moves, the game is forced to terminate. We evaluate them after every 1,000 episodes (evaluation frequency  $E$  in Algorithm 1). Patience  $P$  and tolerance  $\tau$  in Algorithm 1 are 3 and 0.1, respectively. The agents are implemented using PyTorch [30].

### E.3 Wall Clock Time

We report our experiments’ wall clock time. We run all the experiments on single NVIDIA P40/P100 GPUs.

Table 9: Wall clock time for all experiments.

Setting/Component	Batch Size	Approximate Time
GATA		
Graph Updater - OG (Section 3.2)	48	2 days
Graph Updater - COC (Section 3.2)	64	2 days
Action Scorer (Section 3.3)	64 (backprop)	2 days
GATA-GTP		
Discrete Graph Updater (Appendix C.2)	128	2 day
Action Scorer (same as (Section 3.3))	64 (backprop)	2 days
GATA-GTF		
Action Scorer (same as (Section 3.3))	64 (backprop)	2 days
Discrete Graph Encoder Pre-training		
Action Prediction w/ full graph, for GATA-GTF (Appendix C.3)	256	2 days
Action Prediction w/ seen graph, for GATA-GTP (Appendix C.3)	256	2 days
State Prediction w/ full graph, for GATA-GTF (Appendix C.3)	48	5 days
State Prediction w/ seen graph, for GATA-GTP (Appendix C.3)	48	5 days
Deep Graph Infomax w/ full graph, for GATA-GTF (Appendix C.3)	256	1 day
Deep Graph Infomax w/ seen graph, for GATA-GTP (Appendix C.3)	256	1 day
Text-based Baselines		
Tr-DQN (Section 4.1)	64 (backprop)	2 days
Tr-DRQN (Section 4.1)	64 (backprop)	2 days
Tr-DRQN+ (Section 4.1)	64 (backprop)	2 days



